The role of neo-tectonics in the sedimentary infilling and geomorphological evolution of the Guadalquivir estuary (Gulf of Cadiz, SW Spain) during the Holocene

Antonio Rodríguez-Ramírez [a], Enrique Flores-Hurtado [b], Carmen Contreras [a], Juan J. R. Villarías-Robles [c], Gonzalo Jiménez-Moreno [d], José Noel Pérez-Asensio [e], José Antonio López-Sáez [f], Sebastián Celestino-Pérez [g], Enrique Cerrillo-Cuenca [g] & Ángel León [h]

[a] Departamento de Geodinámica y Paleontología. Universidad de Huelva. Campus de Excelencia Internacional del Mar, CEIMAR. Avenida 3 de Marzo, s/n 21007 Huelva (España). arodri@uhu.es

[b] Espacio Natural de Doñana. Junta de Andalucía. Ctra. El Rocío-Matalascañas, 21760 Almonte (Huelva, España).

[c] Instituto de Lengua, Literatura y Antropología. Centro de Ciencias Humanas y Sociales (CCHS). Consejo Superior de Investigaciones Científicas (CSIC). Calle Albasanz, 26-28. 28037 Madrid (España).

[d] Departamento de Estratigrafía y Paleontología. Facultad de Ciencias. Universidad de Granada. Avda. Fuentenueva S/N. 18002 Granada (España).

[e] Earth and Environmental Science Section. University of Geneva. Rue des Maraîchers 13, 1205, Geneva (Switzerland).

[f] Instituto de Historia. Centro de Ciencias Humanas y Sociales (CCHS). Consejo Superior de Investigaciones Científicas (CSIC). Calle Albasanz, 26-28. 28037 Madrid (España).

[g] Instituto de Arqueología de Mérida. Consejo Superior de Investigaciones Científicas (CSIC). Plaza de España 15, 06800, Mérida (España).

[h] Fundación del Hogar del Empleado (FUHEM), Colegio Lourdes. C/ San Roberto, 8. 28011 Madrid (España).

Abstract

A multidisciplinary analysis of cores and geomorphic patterns in the marshes of Doñana National Park (SW Spain) has yielded new evidence regarding the sedimentary infilling and geomorphological evolution of the Guadalquivir estuary during the Holocene. The sedimentation and geomorphological disposition have been strongly conditioned by neotectonic activity along a set of SW-NE alignments, interrupted by other alignments that follow E-W and NW-SE directions. The most conspicuous of the SW-NE alignments is the Torre Carbonero-Marilópez Fault (TCMF). South of this fault, the estuary experienced a marked subsidence from about 4000 to 2000 cal. yr BP through a series of sedimentary sequences of retrogradation and aggradation within the context of relative sea-level rise. From c. 2000 cal. yr BP to the present the subsidence has remained relatively dormant, with progradation of the littoral systems and infilling of the marshland progressing within a context of sea-level stability. Our results reveal that neotectonic activity is a critical factor that must also be reckoned with in any attempt to understand the Holocene geomorphological evolution in the Guadalquivir estuary.

Key words: Sedimentary infilling, Estuarine facies, Holocene, Neotectonics, Guadalquivir estuary, South-west Spain.

1. Introduction

It is well known that estuaries evolve as the result of the interaction between geomorphological structures and dynamic processes that are marine as well as riverine; this interaction adds up to processes that are inherently estuarine. Local modifications also intervene; they derive from relative sea-level changes, climate conditions and human activities (Jackson, 2013). Neotectonic activity (hereafter referred to as

neotectonics) ought to be included as a factor as well; in combination with the other parameters, it may cause changes in the sedimentation rates, result in the creation of new geomorphological features (spits, dunes, cheniers, marshes, levees, alluvial soils), sea-level oscillations (Kennedy, 2011; Yeager et al., 2012; Feagín et al., 2013) and associated tsunami and storm inundation (Morton et al., 2007; Nichol et al., 2007). The subsidence lowers tidal salt-marshes and fertile lowlands below the level of the sea, which thereafter deposits layers of sediments on the former sub-aerial surfaces until fresh alluvial sedimentation overrides these layers, only to be buried below sea level in the next subsidence cycle (Bolt, 2003). Because of relatively rapid developments such as these, neotectonics must be taken into account in any geomorphic and sedimentological analysis that aims to reconstruct past environmental evolutions in littoral areas close to zones of contact between tectonic plates (Rey & Fumanal, 1996; Ulug et al., 2005).

The Mediterranean basin presents numerous examples of neo-tectonic activity that conditions the morphodynamic evolution of the coastlines, specifically vertical displacements related to the collision of the African and Eurasian plates; as in Apulia, Italy (Mastronuzzi & Sansó, 2012), the south-east of the Aegean Sea (Ulug et al., 2005), and the Gibraltar Strait (Zazo et al., 1999c). Comparable scenarios have been identified along the Pacific coasts of North and South America (Atwater et al., 1992; Muhs et al., 1992; Bolt, 2003; Ota et al., 2004). In North America, for instance, cycles of subsidence of the coastline have been reconstructed in connection with the punctuated downward movement of the North American plate vis-à-vis the Pacific plate in the Cascadian subduction zone (Nelson et al., 2006; Shennan et al., 2006). Across the Western hemisphere, in the Gulf of Mexico, active fault motion has been suggested as a prime mover of the recent evolution of the coastline (Yeager et al., 2012; Feagín et al., 2013).

The multidisciplinary examination of cores extracted from estuaries, lagoons, salt-marshes, coastal barriers and deltas has revealed a great deal of information about these evolutions (Vött, 2007; Sorrel et al., 2009).

In the present paper we offer the results of a comprehensive geological study of the geomorphological patterns recognized in the Guadalquivir estuary, which have been poorly researched to date. The study included continuous core-drilling and subsequent lithostratigraphic, paleontological and mineralogical analyses, as well as archaeological probing and radiocarbon determinations. We contend that sustained neotectonic activity in the estuary, as in geologically comparable areas elsewhere in the world, has contributed significantly to the sedimentary infilling and geomorphological configuration of the basin during the Holocene, marking it out from the other estuaries in the Gulf of Cadiz. Our results, in effect, indicate that neotectonics has been a critical factor in the evolution of the entire Atlantic–Mediterranean linkage coast after the transgressive maximum of the Atlantic Ocean; consequently, it must be so taken into account in any future understanding of such evolution. We aim primarily at defining a new palaeogeographic framework in which to ground fresh multidisciplinary research in an area, such as Doñana National Park and its environs, that is so internationally attractive from a natural as well as a cultural standpoint.

2. Geological and morphodynamic setting

The Iberian Peninsula lies at the southwest corner of the continental component of the Eurasian plate, right across the northern boundary of the African plate or Azores-

Gibraltar fault zone. The present geological structure of the Gulf of Cadiz is the result of the European–African plate convergence motion, dextral strike-slip along the Azores–Gibraltar Plate Boundary (Medialdea et al., 2009). This plate convergence lasted from Mid Oligocene up to Late Miocene times and then continued with slow Late Miocene to Recent NW convergence (Rosenbaum *et al*., 2002). Westward drift and collision of the North African and southern Iberian margins in the Early–Middle Miocene caused the radial emplacement of huge allochthonous masses (the so-called "Olistostrome Unit") in the Guadalquivir Basin (Iberian foreland) and the Gulf of Cadiz (Torelli et al., 1997; Maldonado et al., 1999). Such emplacement on the Atlantic realm has been related to the western migration of the Alborán terrain as a consequence of a once active subduction zone (Royden, 1993; Iribarren et al., 2007). Alternatively, Gutscher et al. (2002) proposed that this subduction is still active. This complex geodynamic evolution is recorded in the architecture and tectonic structure of the continental margin of the Gulf of Cadiz and likely in the sedimentary infilling and geomorphological evolution of the littoral landforms. In connection with neotectonic activity in the area, tsunamis—occasionally of rather large magnitude—are a type of high-energy event that affects the Gulf. There is a large body of data on this type of event occurring periodically over the past 7000 years (Lario et al., 2011).

The Gulf includes a number of estuaries, all of them partly enclosed by coastal barriers or spits. Borings taken at some of the largest of these estuaries have provided cores that are the basis for the current understanding of the sedimentary evolution of this coast of southwest Iberia during the Late Pleistocene as well as in the Holocene. The most consistent and reliable results to date have been obtained from borings done in the estuaries of the Guadalete and Odiel-Tinto rivers (Goy et al., 1996; Dabrio et al., 1999,

2000; Borrego et al., 1999). Yet the largest estuary in the Gulf, by far, is the estuary of the Guadalquivir River, enclosed by two spits (Doñana and La Algaida) (see Fig. 1). The entire area encompasses one of the largest wetlands (50,720ha) in Europe as well as Doñana National Park, a UNESCOMAB Biosphere Reserve. Paradoxically enough, the infilling of this large basin in the course of the Holocene has drawn but scant interest. Significant contributions have only been a fragmentary analysis of a long core (Zazo et al., 1999a; Lario et al., 2001; Pozo et al., 2010) and research on the period between the Upper Pliocene and the Quaternary which has failed to concentrate on the evolution during the Holocene (Salvany et al., 2011).

Paucity of dated cores has combined with a complex tectonic activity in the basin to render reconstructions of the fossil infill difficult (Zazo et al., 2008; Rodríguez-Ramírez et al., 2012). Research on the Holocene features has mostly addressed the geomorphology of the surface formations, although it has resulted in a number of models of palaeoclimates, palaeoenvironments and sea-level fluctuations charted on a sound chronological database (Menanteau, 1979; Zazo et al., 1994; Rodríguez-Ramírez et al., 1996; Rodríguez-Ramírez, 1998; Lario et al., 2001; Ruiz et al., 2004, 2005; Rodríguez-Ramírez & Yáñez, 2008). The same formations have been pointed out to in the search for pre-Roman archaeological sites in the estuary and its vicinity (Bonsor, 1922, 1928; Fernández Amador de los Ríos, 1925; Schulten, 1945; Corzo, 1984; Kühne, 2004). The chronological database elucidates a number of periods of climate, natural environment and sea-level changes, as well as phases of progradation and erosion of beaches, that unfolded after the transgressive maximum of the Atlantic Ocean c. 6500 ^{14}C yr BP (Zazo et al., 1994). As refined from studies of spit systems elsewhere in southern Iberia, on the Mediterranean as well as on the Atlantic seaboard (Lario et al.,

1995, 2001; Goy et al., 1996, 2003; Rodríguez-Ramírez et al., 1996; Dabrio et al., 1999; Ruiz et al., 2004, 2005; Zazo et al., 1994, 2008), the database now includes as many as six discrete phases of progradation (H_1 to H_6) following such a transgressive maximum, each phase separated from the next by an erosive surface or a particularly large swale, or both, known as a "gap." Oddly enough, the subaerial record in the spit system of Doñana—the most extensive in the Gulf of Cadiz, fronting the Guadalquivir estuary—and that of La Algaida register only part of the H_5 phase (the oldest beach ridges exposed having been dated to c. 2000 cal. yr BP) plus the entire H_6 phase, from c. 500 cal. yr BP to the present (Zazo et al., 1994; Rodríguez-Ramírez et al., 1996). Evidence of phases H_1, H_2, H_3 and H_4 is missing. In stark contrast, the Guadalete and Tinto-Odiel estuaries present exposed prograding units from the H_3 phase to the present (Goy et al., 1996; Dabrio et al., 2000; Zazo et al., 2006, 2008) (Fig. 2).

Behind the Doñana spit system sits a large marshland area (185,000ha)—the heart of the Guadalquivir estuary—that is the end product of the sedimentary infilling of the original Holocene basin or palaeoestuary by the Guadalquivir and other rivers, a process that developed in the manner of a finger-like delta formation extending in a low energy environment favoured by the growth of the large littoral barriers that isolated the palaeoestuary from the sea (Rodríguez-Ramírez et al., 1996; Rodríguez-Ramírez, 1998). With a low gradient, features in the marshland include various muddy morphologies (levees, channels, point-bars) that have resulted from intense fluvial action, extensive sandy and shelly ridges (cheniers) resting on the clayey sediments, and marine processes operating against the barriers (Rodríguez-Ramírez et al., 1996). The wide-ranging chenier plain formed during two phases of accumulation: from c. 4200 to 2800 cal. yr BP and from c. 1400 to 1000 cal. yr BP (Rodríguez-Ramírez & Yáñez, 2008).

No surface landforms of the same characteristics dating to a phase in between, of some 1400 to 2800 yr BP, have been encountered (Rodríguez-Ramírez & Yáñez, 2008). The reason for this anomaly must be found in the tectonic complexity that affects the Holocene features.

Beneath the marshland sediments, Plio-Quaternary deposits as much as 300m thick unconformably cover Late Miocene-Early Pliocene blue marls (Salvany & Custodio, 1995) as well as the Olistostrome. As remarked by Armijo et al. (1977) and Viguier (1977), the geomorphological and stratigraphic architecture of such deposits furnish evidence of neotectonic activity at least up to the Late Pleistocene along normal faults, favoring "domino tectonics" that governs the drainage pattern of the rivers and the coastline as known today. The same authors identified in the structure of the Plio-Quaternary deposits of the lower Guadalquivir basin two sets of normal faults linked to an assumed Pliocene extensional phase: a main set of N–S oriented faults that includes the lower Guadalquivir and Guadiamar-Matalascañas faults (BGF and GMF, respectively) and a subordinate system of E–W oriented faults that mainly developed in the westernmost part of the basin (see Fig. 1). Later studies by Goy et al. (1994, 1996), Salvany & Custodio (1995) and Zazo *et al.* (2005) have described comparable E-W oriented faults—such as those of Torre del Loro (TLF) and Hato Blanco (HBF)—that shape the more recent sedimentation in the Huelva coast during the Pleistocene (Fig. 1). Furthermore, studies by Flores-Hurtado (1993) and Salvany (2004) have identified NW-SE and NE-SW oriented systems of alignments and a regional tilting of the basin toward the SSE as the dominant structural features that impinge upon the sedimentation. The submerged shelf of the Gulf of Cadiz is also criss-crossed by a system of

alignments, most of which are NE–SW and NW–SE oriented; these alignments nurture mud volcanoes and diapiric processes (Medialdea et al., 2009).

3. Materials and methods

3.1. Geomorphology

We analyzed by photo-interpretation aerial photographs taken in 1956 (1:33,000), 1998 (1:10,000), and 2010 (1:10,000) in order to define the geomorphology of the sedimentary bodies, including the anomalies in the geomorphology caused by the rivers and the vegetation. The initial cartography of the resultant morphologies was complemented by direct observations in the field.

The Topographic Map of Andalusia (1:10,000) served as a base document for mapping. More detailed topographic information, obtained by Light Detection and Ranging (LiDAR) surveying, made it possible to inspect at closer, centimetre-scale the formations in the marshland. This information was checked with the said series of aerial photographs by using a Geographic Information Systems program, gvSIG.

3.2. Lithostratigraphy

The investigation for this paper concerns the sedimentary sequence registered in 5 cores, of depths ranging from 4 to 18m (MA, S6, S8, S9 and S11 (Fig. 1)), all but one of which obtained between 2006 and 2010. We also examined the uppermost section—pertaining to the Holocene formations—of 5 other cores (ML, PN, TC, CM2 and CM3 (Fig. 1)) that the Geological and Mining Institute of Spain (IGME) had drilled in the

area previously; the borings were taken mainly by a direct circulation rotary method, with continuous core sampling (Cruse, 1979) (see Table 1). In addition, we relied on a number of shallow (< 3 m) test trenches and pits (CV, LSM (Fig. 1)) dug in surface formations by means of a 2cm diameter Eijkelkamp gouge and an 8cm diameter helicoidal drill.

The aim was to identify the morphology, geometry and extension of the sedimentary bodies, as well as the relationship they bear with underlying and overlying sediments. The stratigraphy and lithology of each core was described during field sampling. Grain-size distributions were determined by wet sieving for the coarser fractions (>100mm); for fractions lesser than 100mm, grain-size analysis required photosedimentation on a Mastersizer 2000 laser diffractometer ("Sedigraph 5100").

3.3. Palaeontology

A general revision of the taxonomical determination as well as the estimation of densities and diversities of species (faunal composition and shell taphonomy) was possible by means of a macrofossil analysis. Samples of the formations were collected and prepared by washing the bulk sediment (12 cm^3) through a 1mm sieve. Bivalves and gastropods were identified to the species level and then counted to determine the semi-quantitative distribution of the species in each core. The presence and relative abundance of other groups (scaphopods, barnacles, bryozoans, etc.) were also noted.

3.4 Mineralogy

Mineralogical analyses were conducted by powder X-ray diffraction (XRD) techniques on a Bruker-AXS D8-Advance diffractometer, using monochromatic CuKα radiation at 40kV and 30mA. Random powders were scanned from 3 to 65° 2θ at 2° 2θ/min, after gentle grinding and homogenisation to <63μm.

3.5. Dating

Twenty radiocarbon dates were considered relevant to this study. Ten of them apply to samples from mollusc shells which were subjected to the AMS method in the laboratories of Beta Analytic (Miami, USA), Centro Nacional de Aceleradores (Seville, Spain), and Accium BioSciences Accelerator Mass Spectrometry Lab (Seattle, USA). The shells selected were those that showed, wherever possible, a low degree of transport or no transportation, and were preserved as articulated valves in the sedimentary record. The remaining ten dates had been obtained by other authors (see Table 2). Calibration relied on version 6.0 of the CALIB program (Stuiver & Reimer, 1993) as well as on the calibration dataset of Stuiver *et al.* (1998). Correction of the reservoir effect followed A. M. M. Soares's guidelines regarding calibration of marine shells from the Gulf of Cadiz (Soares & Martins, 2010). Expressed in Delta-R (ΔR) values, conditions of the reservoir effect are known to vary over time as well as space. For the Late Holocene on the Andalusian coast of the Gulf of Cadiz, Soares recommended a ΔR value of −135±20 ^{14}C yr; except for the range 4400-4000 ^{14}C yr BP, for which he suggested a value of +100±100 ^{14}C yr (see Soares & Martins, 2010, for details). Lack of sufficient data for the 4,000 to 2,000 ^{14}C yr BP preclude determining with enough assurance the most recent time boundary to which the +100±100 ΔR value can be extended. We chose to extend it to the middle ^{14}C year 3000 BP. New data on reservoir effects are necessary to

calibrate with greater precision samples from the Gulf of Cadiz. Final date estimates in the dataset specify 2σ intervals (see Table 2).

The resultant isotopic determinations were compared with the age of archaeological remains known from the area (Bonsor, 1928; Corzo, 1984; Campos et al., 1993, 2002). In addition, pottery shards were discovered in and extracted from the littoral strands of Carrizosa-Vetalarena; they were sent to Instituto de Arqueología del CSIC (in Mérida, Spain) for typological analysis and dating.

4. Results

4.1. Geomorphology

A detailed cartography highlighting the surface features (spits, dune systems, cheniers, beach ridges, levees and present-day hydrography) reveals a number of clearly distinct geomorphological units (Fig. 1), as described in the following sections.

4.1.1. The Abalario Dune Systems

This remarkable unit, north of the research area, comprises different semi-stable dune systems that move in NW and W directions. The dunes can be as high as 70m above sea level. Marine erosion results in cliffs that are 10 to 15m high. Altitudes decrease according to a north to south pattern. South and east, the dune formations gradually fossilize below the present-day marshes and the Doñana spit. Lagoon environments, in

association with dune fronts and deflationary basins, have developed in between, generating notable wetlands.

4.1.2. Dunes in the spits

Overlying the Abalario unit and the marshland, this spectacular complex includes two systems already mentioned: Doñana and La Algaida. The two systems are connected to the prograding phases of the coast. The most recent dunes (conspicuous in the Doñana spit) have developed from being foredunes to becoming well-formed transversal bodies, as much as 30m high. Below this transversal system lies a second one toward the inner side of the estuary; the dunes here are lower—no more than 10m high—and have evolved into parabolic dunes. This lower system constitutes the central area of the La Algaida spit.

4.1.3. Littoral strands in the spits

Identified and mapped in the southernmost—i.e., most recent—sector of the Doñana spit, these successive, overlapping landforms signify an intense progradation of the coast. The strands, 4 to 7m high, have accumulated in a S-SE direction; some are covered by foredunes. Out of a total of 21 strands, the first six curve toward the west, while the rest, beginning from an erosive line, do so toward the east. Although the spit shows a marked alternation between ridges and swales overall, the dunes covering the most recent strands hide this alternation. On the La Algaida spit, the littoral strand surrounds the central area and connects with the mainland in the form of a tombolo.

4.1.4. Marshland levees

Part of a deltaic system that has been filling the estuary, these clay-rich levees flanking the Guadalquivir River and its relict beds have a variable width (300 to 2,000m) and a great length. They can reach heights of 0.5 to 1.8m above the adjacent inter-levee marshes or flooded areas. Altitude diminishes progressively from north—2m—to south—0.5 to 1m near the mouth of the river—on a slope with a gradient of 0.004%. As we shall see, two different sectors can be distinguished, each with a distinct configuration.

4.1.5. Cheniers

Sandy and shelly deposits with a littoral strand morphology overlie the clayey infilling of the marshland, their original shape having been blurred by the activity of the fluvial network. The sandy formations of Carrizosa-Vetalarena and Vetalengua are distally attached to the Doñana spit and oriented toward the NE over long distances; in the case of Carrizosa-Vetalarena, as much as 10km (Fig. 1). These formations, 50 to 100m wide and 2.15 to 2.25m high above sea level, consist of overlapped strands. The cheniers are deposits of abundant, almost exclusive mollusc shells, chiefly shells of *Cerastoderma edule*; those of Marilópez and Las Nuevas stand on the south-west banks of the marshland levees and on sandy formations. Their morphology is that of beach formations, with narrow, small ridges and landward-dipping crests. At points S6 and PN, the sandy and shelly deposits found in the uppermost section of the cores belong in the littoral strand system of Carrizosa-Vetalarena and the chenier of Las Nuevas, respectively.

4.2. Geomorphological anomalies.

Detailed analysis of the aerial photographs and satellite images, LiDAR information and topographic maps enabled us to identify a number of geomorphological anomalies, such as peculiar drainages, subdued morphologies, erosive forms, even patches of vegetation caused by weaknesses and changes of humidity in the ground.

Remarkably orthogonal, rectilinear alignments marked by the hydrographical network stand out in SW-NE (≈N50-60E) and NW-SE (≈N110-130E) directions (Fig. 3). These directions, which define the northern and southern boundaries of the marshland area, match the directions of the Neogene formations located farther north (Fig. 1). Two topographical sections (C-D and A-B) reveal sharp level differences of 10 to 30cm (Fig. 4). Seemingly not much of a topographic gradient in such an extensive area, the abruptness of the offset makes it significant.

The erosive inflection of El Puntal also calls the observer's attention, as does its projection along the Carrizosa-Vetalarena sandy ridge in the same SW-NE direction (Figs. 1, 3). Such alignment cuts through the right-hand levee of the Guadiamar channel, leaving toward the north a surface of old marshland—rather degraded at some locations (Fig. 5)—which rises 1.80m over the surrounding plain. South of the alignment, the levees show a different arrangement: much more developed longitudinally than transversally. In addition, there are remnants of block-like surfaces that exhibit an odd drainage pattern (Fig. 3): a sign of probable tilting in a southerly direction.

4.3. Lithostratigraphic, paleontological and mineralogical analyses of the cores

The cores exposed a series of Holocene deposits (in marshland, dunes and beaches) resting on pre-Holocene formations of sands and clays that indicate dunes and marshes (Fig. 6 and Table 3):

4.3.1. Pre-Holocene Marshland Formation (PHMF)

A substratum for the subsequent Holocene deposits, this facies of grayish ochre (10YR8/2) silts turned up in cores S11, ML, and PN at depths of -13, -11 and -28m, respectively. The silts make up 0-75%; clay, 20-25%; sand, 2-5%. Burrowing, roots, carbonate nodules, oxidation, and intense lamination were found. Macrofauna were absent. Detrital minerals (quartz, feldspar) amounted to 6-10% and 2-4%, respectively. Calcite (15-35%), filosilicates (50-70%), and traces of dolomite (7%) were also encountered.

4.3.2. Abalario Dune Formations (ADF)

White-orange (10YR8/6), reddish-tinted (5YR6/8) sands, lightly crusted at some points, appeared in cores TC, S6, S9 and MA at -19, -11, -7 and 0m, respectively. At the MA point, the top of the dune formation is present at sea level, surfacing as a result of wave-induced coastal erosion and becoming fossilized under the current beach deposits and foredunes. The plane of contact between the ADF formations and the subsequent

Holocene deposits leans progressively toward the south, down to -19m at the TC location.

Lithostratigraphic analysis revealed 75-90% sand, 5-20% silt and 1-4% clay. The sand is made of well rounded, well sorted grains, 65% of which measure from 250 to 1000µm. Mineralogical analysis yielded 75-95% quartz, 5-14% feldspar, 8-10% filosilicates and 2-3% dolomite. No remains of macrofauna were encountered. On a regional scale, the sequence has a thickness of as much as 100m (Salvany et al., 2011). North of the study area, marine erosion of the formation has resulted in a cliff 15 to 20m high, where one can identify several aeolian sequences that contain traces of dune slacks in the form of peats. These peats have been dated to the Upper Pleistocene (Zazo et al., 1999b, 2008).

4.3.3. Holocene Estuarine Formation (HEF)

The thickness of these deposits turned out to vary greatly according to the location chosen for the drilling. At point S9 the thickness is some 6 m below ground; at S6, S8, S11 and ML, it is between 11 and 13m; at PN, as much as 28 m. The ground surface at all these points stands roughly 1 to 2.5m above sea level. At CM3 and CM2, where the sedimentary record is more discontinuous, the ground surface is 6m above sea level (Table 3).

In the inner, central part of the estuary, the prevalent lithology is one of grey (5Y 8/2) clayey silts (Table 3), with some sand: 65-75% silt, 20-30% clay, 0-6% sand. The sand decreases gradually toward the top of the sedimentary sequence. Macrofauna are

present: mostly *Tellina tenuis*, *Cerastoderma edule* and *Crassostrea angulata*, the remains decreasing toward the top. The top 1m registered the prevalence of terrestrial, freshwater species (*Cochlicella, Helix, Melanopsis*). Burrowing and lamination were also found, with stems and roots in the top. The mineralogical analysis revealed an abundant presence of filosilicates (60-80%) and lesser amounts of quartz (10-30%), calcite (5-20%), feldspar (3-10%) and dolomite (2-5%).

In outer sub-areas of the estuary, such as the Doñana spit, cores CM3 and CM2 yielded successive deposits of estuarine facies separated from one another by intervals of the sandy facies of the HSF, described below (Fig. 6). Because of the greater marine influence in the Doñana spit, at CM3 and CM2 such sandy facies contained sandy silts made of grains coarser (10-30% fine sand, 30-40% silt, 10-15% clay) than those found in the cores from the central part of the estuary (Table 3). The intervals—consisting of quartz (10-20%), filosilicates (30-50%) and calcite (15-20%)—had burrows, roots and lamination, as well as remains of transported marine malacofauna (*Glycimeris* sp., *Ostrea* sp.) and estuarine species (*Cerastoderma edule, Tellina tenuis*) showing a low degree of transport or no transport

Interspersed with the silt sequences were also facies of sandy layers (40-70% sand, 25-40% silt, 5-10% clay) (Table 3) that resulted from erosive interruptions in the sedimentary build-up of the estuary caused by high energy events such as storm surges or tsunamis. The thickness of these sandy facies ranges from a few decimeters at some locations to over 1m at others. The mineralogical composition is largely quartz (50-95%), complemented with filosilicates (10-40%), feldspar (10%) and dolomite (10-15%). Palaeontological remains concern species as highly diverse as *Chlamys*

multistriata, Chlamys flexuosa, Venus sp., Glycymeris sp., Chamelea gallina, Murex brandaris, Solen marginatus, Cerastoderma edule, Crassostrea angulata and *Tellina sp.* One of these marine erosion-related, sandy deposits, of varying depth—and turning into silt sediments toward the top—marks the entire HEF sedimentation from the facies that underlie it (ADF and PHMF). At S9 these deposits clearly indicate an erosive event as they contain a massive accumulation of shells (both articulated bivalves and disarticulated valves) and shell fragments in a sandy-muddy matrix with gravel and lithoclasts on an erosive base on top of ADF. At S6 this facies constitutes the top of the core, which corresponds to the Carrizosa-Vetalarena littoral strand, mentioned above, extending over many kilometres farther inland through marshland (Fig. 1). At point CV, farther south, a different, more recent sandy facies makes up Vetalengua, the other littoral strand system that is part of the Doñana chenier plain.

Other sediments in the HEF consist of layers of bioclasts (Table 3) of malacofauna (mostly *Cerastoderma edule* and *Crassostrea angulata*) in a grey (5Y 8/2) silt-clayish matrix containing some sand (40-60% silt, 25-30% clay, 10-30% sand). The mineral content consists of filosilicates (50-70%) with lesser amounts of quartz (10-20%) and calcite (15-25%). At PNL the very top of the core turned out to have a littoral strand morphology that also spreads at length over the marshland area, as part of the large chenier of Las Nuevas.

4.3.4. Holocene Spit Formations (HSF)

These facies are clearly represented at points TC, CM2 and CM3 by siliceous sands that indicate dune events and beaches (Table 3).

At TC, CM2 and CM3, sands documenting dune accretion turned up in the top 2.5, 3 and 3.5m, respectively, of the core, corresponding to the present foredunes. At CM3, the two sand layers—found from the top down to -8m and from -14m to -18m—exhibit a composition that is homologous to that of the present dunes. They are yellow (10Y8/6) fine-to-medium-grained sands, very well sorted and rounded. As much as 55% of the sediment exhibits a mean grain size of 125 to 500μm. The sediment includes mostly quartz (70-85%) with filosilicates (15-25%) and feldspars (5-10%); with no macrofossils.

Sands indicating beaches are ochre-yellowish (2.5 7/6), fine-to-coarse-grained sands, poorly sorted (Table 3). The TC core yielded a continuous record with coarser deposits, including coarse pebbles. At CM2 these sand intervals appeared in succession throughout the core, each interval separated from the next by an estuarine facies (Fig. 6). Calcite (10-15%), filosilicates (10-20%), feldspars (15-25%) and especially quartz (40-55%) made up the mineralogical composition. The sands contained paleontological remains. A wide diversity of species of malacofauna, rather deteriorated by a high degree of transportation, was identified: *Chlamys multistriata*, *Cymbium olla*, *Panopea sp.*, *Chlamys flexuosa*, *Venus sp.*, *Glycymeris sp.*, *Murex brandaris*, *Venus sp.*, *Tapes sp.*, *Chamelea gallina and Solen marginatus*. The record at LSM, on a littoral strand of the Doñana spit, corresponds to such facies in the top of the CM2 core.

4.4. Chronology

As noted above, twenty ^{14}C dates were considered for the study, ten of which we ourselves had obtained in the course of the investigation (Table 2). The oldest formation detected in the cores was the Pre-Holocene Marshland Formation (PHMF), with radiocarbon ages ranging from 19,000 BP to > 47,000 BP. Point S11 yielded a radiocarbon age of 19,360±80 BP at a depth of -13m, the top there of the PHMF. Point PN produced an age of >46,000 BP at a depth of -35.5m; point ML, an age of >47,000 BP at -27m. All of these radiocarbon determinations could not be calibrated, as they are out of range for the calibration.

The remaining radiocarbon determinations, from c. 8000 cal. yr BP up to the present, pertain to facies of the Holocene Spit Formations (HSF) and the Holocene Estuarine Formation (HEF). In all the cores analyzed, formations HSF and HEF appeared consistently overlying both the PHMF and the Abalario Dune formations (ADF); furthermore, in all the cores drilled in the inner estuary (S6, S8, S9, PN and ML) the HEF appeared to start with a high-energy sand deposit containing abundant marine fauna, from which we collected most samples for ^{14}C dating.

Point PN yielded the oldest radiocarbon determination for the HEF: 6543-6789 cal. yr BP. In contrast, points S11, S6 and ML place the earliest Holocene sedimentation in the years 5255-5461 cal. yr BP, 5693-5910 cal. yr BP and 5728-6012 cal. yr BP, respectively. At S9 the date obtained for the same facies is more recent: 3830-4410 cal. yr BP. At TC the Holocene Spit Formations (HSF) produced as early a date as 7793-8116 cal. yr BP.

The emerged formations with the oldest ^{14}C dates are the littoral strands of Carrizosa-Vetalarena (at point S6), 4071-4706 cal. yr BP, and Vetalengua (at point CV), to the south of the former, 1825-2149 cal. yr BP. As remarked above, both Carrizosa-Vetalarena and Vetalengua are part of a chenier plain system formed within the estuary. As to the perimeter of the Doñana spit, the oldest littoral strands known (at point LSM) produced a date as recent as 1883-2152 cal. yr BP; there, strands are the same as those that cap the sedimentary record at CM2.

The ^{14}C dates obtained were in accord with the age of archaeological remains encountered in the area. The top of CM3 is closely related to remains from the 2nd to the 6th century CE (Bonsor, 1928; Campos et al., 2002). The pottery shards extracted from the littoral strands of Carrizosa-Vetalarena date from the late Neolithic and Copper Age in south-west Spain (roughly 5,500 to 4,000 cal. yr BP). Neolithic and Copper Age finds are also known from large tracts north and north-west of such strands, within the present-day geomorphological area of El Abalario (Campos et al., 1993; Campos & Gómez-Toscano, 1997).

5. Discussion

5.1. Pre-Holocene formations

The ten cores selected register a pre-Holocene substratum of qualitatively distinct material (PHMF and ADF formations) at a varying depth. In the cores TC, S6, S9 and MA, it is the ADF (Abalario Dune Formations) that constitutes this substratum. The different depths at which these dune formations appear—-19m, -11m, -7m and 0m,

respectively—indicate a progressive, non-synchronous sinking of the ADF toward the south.

To the north, within the present-day geomorphological area of El Abalario (Fig. 1), the ADF has been subject to especially destructive coastal erosion, the effect of which being the generation of a large cliff there. By studying the position of a number of 16th- and 17th-century watchtowers in the area vis-à-vis the shoreline, a rate of cliff recession of 0.7 to 0.8m/yr on average has been calculated for the La Higuera watchtower, near the MA location (Fig. 1). To get some idea of the approximate coastal recession accrued there over longer time spans, one can apply such rate to the past 2500 and 5000 years, obtaining as a result that the shoreline may have receded as much as 1800 m and 3600 m, respectively, since the mid Holocene.

Laterally toward the centre of the estuary, the ADF seems to interdigitate somehow—no reliable data are available to describe it—with the PHMF formation, as the latter appears at points S11, ML and PN at depths of -13, -11 and -28m, respectively. The presence in the PHMF deposits at these locations of burrowing, roots, carbonate nodules and intense lamination suggests either an emerged environment or an environment in transition—subject to periodic tidal inundation as well as freshwater inputs—that the microfauna (Pozo et al., 2010) as well as the pollen (Zazo et al., 1999a) have indicated.

These data about the ADF substratum and the PHMF formation suggest a landscape in the estuary right before the first Holocene deposits that consisted of a shoreline extending far seaward from its present position and made up of a prominent aeolian system. Research on the sedimentary record in the area of El Abalario (Zazo et al.,

2005) substantiates this reconstruction further. Toward the east, the ADF would turn into a muddy alluvial plain (PHMF) which would show clear signs of becoming terrestrialized (Fig. 7A). Numerous archaeological artifacts found spread on the surface across El Abalario (Campos et al., 1993; Campos & Gómez-Toscano, 1997) are evidence of significant cultural activity in the area in the Neolithic and the Copper Age. The pollen record from the current coasts of southwestern Iberia for the period of ≈10,020±50 to 5380±50 ^{14}C yr BP suggests a wet, temperate climate (Santos et al., 2003, who failed to calibrate the radiocarbon determinations they adduced). During this period (the Holocene Climatic Optimum) to judge from the record in the estuaries of southern Spain (Dabrio et al., 2000) and Portugal (Boski et al., 2001), the level of the sea rose rapidly at a rate of 5.7 to 8mm/yr. The end of this humid period has been connected with the Holocene transgressive maximum and, thereby, with the highest level of area flooded (Zazo et al., 1994). After the Holocene maximum, aeolian dune systems started to accumulate, particularly from 6,000–5,000 cal. yr BP onward (Zazo et al., 2008).

5.2. Retro-aggradational Holocene systems

The first morpho-sedimentary units of the Holocene in the Doñana coast took the form of estuarine barriers and marshland at river mouths in relation to sea level. Analysis of the cores indicates that the oldest remnants of such Holocene formations found in the centre of the estuary are those registered in the PN core, dated to 6789-6543 cal. yr BP. Holocene sedimentation would have spread gradually northward from there to reach S6 and ML ≈6000-5700 cal. yr BP (Fig. 7A). Paleontological evidence suggests a lagoon environment at the time under considerable marine influence, including the frequent

effects of high-energy events of sandy sedimentation such as storm surges and the larger, yet more sporadic, effects of tsunamis. Later, as revealed by overlying deposits in the cores, a more confined environment became established, increasingly closed to direct tidal ingress and washover yet open to freshwater inflows from the opposite direction. This evolution has been recognized elsewhere in the estuary by means of the paleontological analysis of other cores (Zazo et al., 1999a; Ruiz et al., 2005; Pozo et al., 2010).

Toward the west (point TC) and south (points CM2 and CM3), in the outer margins of the estuary, the earliest evidence of Holocene deposits are those of the Spit Formations (HSF). Made of dunes and beaches that date from 8116-7793 cal. yr BP at a depth of 20 m at TC, such deposits substantiate the formation of a sandy barrier at the beginning of the Holocene that enclosed part of the estuary and, consequently, enabled sedimentation therein of finer materials (Fig. 7A). The core at CM2 exposed an alternation between HSF and HEF, which indicates a punctuated succession over the past 5000 years of marine–dominated environments (foreshore and nearshore) against estuarine-dominated environments. At CM3, deposits of two phases of transgressive dunes (6 to -2 m and -8 to -12 m with respect to present sea level) overlie rather shallow estuarine formations, in a manner like present-day systems of transverse dunes encroaching upon the Doñana marshland. On the basis of studies of microfauna, estuarine-dominated intervals have been interpreted as coastal lagoons evolving into shallow brackish marshes (Rodríguez-Vidal et al., 2011). Such sedimentary alternation between shallow estuarine, on the one hand, and foreshore and backshore marine environments, on the other, fits well with a scenario of retro-aggradational systems nurtured by progressive subsidence of the ground surface and relative sea-level rise.

Pollen from the peat of El Acebrón, near the beach resort of Matalascañas, suggests a *dehesa* landscape forming in part of the basin c. 5,000 cal. yr BP. Agriculture would have been practiced there (Stevenson & Harrison, 1992; López-Sáez et al., 2011).

A transitional zone, functioning as a sort of geomorphological threshold, probably under structural control, would have existed between the outer and inner sides of the estuary. The Madre de las Marismas fault system, with a NW-SE direction, would have conditioned a number of blocs and shaped a rising area toward the W and a subsiding area toward the E (Fig. 7A).

Within the period 4500 to 3500 cal. yr BP, such a transitional zone would have submerged. Evidence of a tsunami hitting the Gulf of Cadiz c. 4,000 cal. yr BP has been argued for (Lario et al., 2011), which points to seismic activity in the area at the time. Turbidite deposits in the Southwestern Portuguese Margin related to a local earthquake c. 3600 cal. yr BP have been reported as well (Vizcaíno et al., 2006). Because of the submersion of the transitional zone, sandy deposits encountered in cores S9 and S8 and dated to 4410-3832 cal. yr BP and 4065-3489 cal. yr BP, respectively, would have buried and fossilized the existing dune formations of El Abalario (ADF) as under a large overwash fan introduced into the inner estuary. The exposed geomorphological evidence of this overwash fan is the littoral strands of Carrizosa-Vetalarena, dated to 4706-4071 cal. yr BP. Clearly laid down by a high-energy event, these marine sands are evidence of both rupture of the littoral barrier that had formed up to that date and notable transgression of the sea into the basin (Fig. 7B). The rapidly submerged, new marine environment can also be inferred from other studies of the area (Rodríguez-Ramírez et al., 1996; Zazo et al., 1999a; Rodríguez-Ramírez & Yáñez 2008). The

effects of this event on the Neolithic and Copper Age settlements in the area must have been considerable, to judge from the numerous archaeological remains found scattered over the wide range of the Abalario dune systems. The pottery shards from the same cultural periods encountered embedded in the littoral stands of Carrizosa-Vetalarena are further indications of the magnitude of the land- and sea-level movement caused by the event (Fig. 7B).

Eventually, an environment of tidal marshland developed in the estuary, as suggested by the renewed build-up toward the west of the littoral barrier. Toward the south (points S8, CM2 and CM3), the thickness of the deposits prevents recognition there of the pre-Holocene substratum; the sandy bottom at S8 appears to be of the same kind as that encountered at S9, however.

A number of studies have enabled specialists to estimate for the Gulf of Cadiz that after the present-day sea level was reached c. 5000 cal. yr BP, the oscillations would not have exceeded 1m since (Zazo et al., 2008). Yet, as we shall see presently, the identification at a varying depth of sediments that are elsewhere part of very shallow landforms (e. g., exposed prograding units) appears to be at odds with the curve of the mean sea level for the Gulf presented by Zazo et al. (as cited), which is the generally accepted curve. Such an anomaly attracts particular attention south of a clear NE-SW structural alignment that we have called the Torre Carbonero-Marilópez Fault (TCMF). This alignment runs parallel to both the Guadiamar-Matalascañas Fault (GMF) (Salvany & Custodio, 1995) and the Lower Guadalquivir Fault (BGF) (Viguier, 1977). North of the TCMF alignment is the Torre del Loro Fault (TLF), where Zazo et al. (1999b) estimated the minimum fault throw on the TLF to be 18 to 20m for the Late Pleistocene (Fig. 1). The

TCMF fault also explains other alignments of lesser morphological expression, especially south of it, as well as noticeable irregularities in the same direction. The TCMF alignment acts as a geomorphological as well as a stratigraphic boundary (Fig 2).

Whereas the dune formations of El Abalario, north of the fault, spread conspicuously over the ground, the corresponding deposits just a few kilometres south of the fault lie buried at ever lower depths (as much as -20m at the TC point). The fault appears intersected at intervals by other lines orthogonal to it, following a NW-SE direction; the most visible are the Madre de las Marismas Fault (MMF) and the Marilópez Fault (MF). Farther north, the significant geomorphological control affecting the fluvial network that drains the Neogene formations, with NW-SE and SW-NE directions, bears witness to the same neotectonic scenario (Flores-Hurtado, 1993) (Fig. 1). Even the coastline itself can be understood as conditioned by related structural alignments, as suggested by the cliffs that have developed in Upper Pleistocene formations to the northwest (Goy et al., 1994; Zazo et al., 1999b). It is commonly accepted that on the coast of the province of Huelva a number of orthogonal fault systems (following NW-SE, NE-SW and E-W directions) outline individual blocks that control swamped areas and elevated areas (Flores-Hurtado, 1993). The received literature (e. g., Zazo et al., 2005; Salvany et al., 2011) registers no indications that such neotectonics could affect formations that are so recent, however.

Following the TCMF alignment, the Carrizosa-Vetalarena littoral strands cross the marshland area to connect with the littoral strand of Marilópez in a chenier system that has been dated to c. 3800-2500 cal. yr BP (Rodríguez-Ramírez & Yáñez, 2008).

Located on the elevated structural margin, these strands define a rather clear geomorphological and palaeogeographic boundary in the marshland area. North of this boundary lies the domain of old marshland, transformed and degraded; south of it, the extension of later systems which have gradually replaced a former tidal lagoon (Fig. 8). Both Carrizosa-Vetalarena and Marilópez outline an ancient shore that remained active for at least 1300 years, as the subsiding section south of the boundary filled up with sediments. The infilling proceeded by way of finger-like deltas (Rodríguez-Ramírez et al., 1996; Rodríguez-Ramírez & Yáñez, 2008) (Fig. 7C, 8).

In short, consistent chronological, stratigraphic and geomorphological data appear to indicate a tilting of the zone south of the TCMF Fault, especially after c. 4000 cal. yr BP. Continental formations (ADF) sunk in the process, to be gradually covered by subsequent estuarine and coastal formations during the course of the Holocene. Because of such subsidence and the corresponding relative rise in sea level, the littoral system saw a series of sedimentary sequences of retrogradation and aggradation during the same time span (Fig. 9).

5.3. Exposed littoral-barrier systems (Progradational systems)

The oldest ages obtained in the exposed beach–barrier systems of the Gulf of Cadiz come from the Valdelagrana spit, which closes the estuary of the Guadalete River. A Middle Bronze Age site found within the spit—dated to c. 3800–3600 BP by Gómez-Ponce et al. (1997) on the typology of some of the archaeological remains encountered; c. 3500 cal. yr BP at the latest—clearly proves that the Valdelagrana system had already built up enough to carry a human settlement by 3500 cal. yr BP if not earlier. Indirect

evidence obtained in other coastal lagoons in SW Spain—e.g., by the spit of Punta Arenillas in the Odiel-Tinto estuary (Zazo et al., 2008)—suggests that the progradation of Atlantic beach–barrier systems had started c. 6,500 cal. yr BP.

Although the Guadalquivir estuary is the largest in the Gulf of Cadiz, the exposed beach–barrier systems in it offering the oldest dates are only those of the littoral strands of Carrizosa-Vetalarena and Marilópez. As remarked above, these strands are located inside the estuary and are part of a chenier plain (Rodríguez-Ramírez *et al.*, 1996; Rodríguez-Ramírez & Yáñez, 2008) (Fig. 1). By contrast, the landforms with the oldest dates in the spit of Doñana are the littoral strands identified at the LSM location, dated to 2152-1883 cal. yr BP, as well as the littoral strand of Vetalengua (CV point) which dates from 2,149-1,825 cal. yr BP. Landforms farther north are made of high piles of dunes, which house remains of a Roman settlement; this settlement was established by a hillock known as "Cerro del Trigo" in the 2nd century CE (Bonsor, 1928; Campos et al., 2002). In the spit of La Algaida, remains of a pre-Roman settlement from the 6th to the 2nd century BC lay buried below the surface (Corzo, 1984) (Fig. 1). Dune systems in both spits have developed cyclically since, thereby reflecting intense progradation toward a sea that had reached its present-day level already, or thereabouts (Rodríguez-Ramírez et al., 1996; Zazo et al., 2008). Analysis of beach ridge morphology, age and distribution reveals that the prograding systems exposed in the spits record part of system H_5 and the entire system H_6. The same analysis provides evidence of periodicity in relation to climatic oscillation and solar activity fluctuation (Zazo et al., 1994; Rodríguez-Ramírez et al., 2000, 2003; Goy et al., 2003). Between 2200 and 1200 cal. yr BP, the formation of a fresh chenier system in the marshland area—namely, Vetalengua-Las Nuevas—accompanied such prograding developments in the spits,

ending up in the final infilling of the palaeoestuary and the displacement of the fluvial network toward the south (Rodríguez-Ramírez & Yáñez, 2008) (Figs. 7D, 9). In such a 1000-year period, the palaeoestuary turned from housing a coastal lagoon—the *Lacus Ligustinus* of Roman times—to encompassing a tidal marsh which eventually became a freshwater marsh. The process made shipping to and from the open sea increasing difficult, which may well explain why the Cerro del Trigo settlement, a fishing and salting-industry town, was abandoned in the 6th century CE.

Whereas indirect data obtained in nearby coastal lagoons of the Gulf of Cadiz (estuaries of Tinto-Odiel and Guadalete rivers) suggest that the progradation of Atlantic beach–barrier systems began c. 6500 cal. yr BP (Zazo et al., 1994; Goy et al., 1996; Dabrio et al., 2000), the said geomorphic and stratigraphic evidence in the Guadalquivir estuary point to the past two millennia as the period within which net progradation in the Doñana spit has developed, in connection with a comparatively stable relative sea level (Fig. 9). Indeed, geomorphic, stratigraphic and chronological analysis of the most recent phases in the growth of this spit, as well as in the formation of chenier systems in the estuary, reveals a relative cessation of the sinking processes—at least south of the TCMF line—in the past 2,000 years or so. Yet between approximately 4000 and 2000 cal. yr BP subsidence was intense there. Relative stability after 2,000 cal. yr BP has resulted in the growth of littoral and dune systems and in the final infilling of the palaeoestuary (Fig. 8). The date 2,000 cal. yr BP is thus a turning point between a retrograding, aggradational system—conditioned by the subsidence-prompted sea-level rise—and a system that progrades in connection with a relatively stable sea level (Fig. 9). This dramatic change of scenario explains the difference between the Guadalquivir estuary and other estuaries in the Gulf of Cadiz: in the former, the growth phases of the

coastal barrier prior to 2,000 cal. yr BP lie buried several metres under the ground surface.

5.4. Mechanisms for the tectonic activity

It is difficult to determine a single mechanism for the tectonic activity that affects the Holocene formations in the Guadalquivir estuary. The forces in operation are the sliding of the Baetic Olistostrome toward the NW and the transpressive tectonics—together with overpressure (fluid escape)—that generates mud volcanoes and diapiric processes in this area of the Gulf of Cadiz. Many structures associated with the fluid escape—including mud volcanoes, mud-carbonate mounds, pockmarks, salt domes and slides—have been identified and characterized in the platform of the Gulf and put in connection with NE–SW and NW–SE alignments (Medialdea et al., 2009), in turn related to the Baetic orogen and the Ibero–African boundary (Maldonado et al., 1999). Growth faults (normal faults with greater sedimentation on the downthrown side) are a common geological feature in sedimentary and deltaic basins around the world (Mauduit & Brun, 1998) and are often located near subsurface reservoirs of hydrocarbon deposits or salt domes (Jackson et al., 1996), as occurs in the Gulf of Cadiz. Fluid overpressure within the Pliocene–Pleistocene sedimentary wedge of coastal plain deposits (Deltaic unit) may have played an important role as well—as it has a little farther north, in the aeolian formations of El Abalario (Zazo et al., 2005; Salvany & Custodio, 1995).

Comparable neotectonic scenarios registered elsewhere in the planet (cycles of subsidence reconstructed for the Cascadian subduction zone (eastern Pacific) and

Japanese coasts (Bolt, 2003), active fault motion in the Gulf of Mexico (Feagín et al., 2013; Yeager et al., 2012)), mentioned earlier, provide some illustrative references for the probable dynamics involved in southern Iberia.

5.5. Archaeological implications

Spanish humanist Antonio de Nebrija, early in the 16th century CE, was perhaps the first who called attention to the extent to which the landscape of the Guadalquivir estuary had changed since Antiquity. A native of the area, Nebrija gave as an example the disappearance of one of the two mouths of the great river—known as '*Baetis'* in Roman times—by the unremitting potency of its alluvial deposits (Nebrija, 1550). In the early 17th century Juan de Mariana (1852-1853) adduced devastating storms and earthquakes to also explain such a geologically rapid transformation.

In the late 19th century historians, linguists and archaeologists began to search the area for material evidence of human settlement in ancient times. The attempts put to public view a large number of archaeological sites, some dated to the prehistory and early history of southern Iberia and others to other periods of history. No doubt the best known of these initiatives was that of archaeologist G. E. Bonsor and linguist A. Schulten at the above-mentioned site by Cerro del Trigo, in the 1920s (Bonsor, 1922, 1928; Schulten, 1945), where Roman remains had been unearthed. O. Jessen, the geologist in the project, found clear evidence of subsidence of the ground surface in the Doñana spit, but could not explain this natural phenomenon (in Schulten, 1945: 272-273). No remains of a pre-Roman settlement ever appeared.

Cerro del Trigo stands on the transgressive dune systems of the Doñana spit (Fig.1). It is the oldest known settlement on the right-hand side of the Guadalquivir estuary. As remarked above, it was a fishing and salting-industry town from the 2nd to the 6th century CE (Campos et al., 2002). For older settlements, one must search as far as the currently visible aeolian systems of El Abalario, to the northwest and off the limits of the spit systems of Doñana (Campos et al., 1993; Campos & Gómez-Toscano, 1997). The reason for such an archaeological gap of the space in between is, clearly, that pre-Roman and older formations in the Doñana barrier are several metres below the ground surface, fossilized by later formations, c. 2000 cal. yr BP old or younger. Possible anthropogenic remains present in such a space can be found by means of indirect survey techniques only.

6. Conclusions

Neotectonic activity appears to have conditioned to a significant extent Holocene sedimentation in the lower Guadalquivir river basin. A set of SW-NE alignments—the most representative of which being the Torre Carbonero-Marilópez Fault (TCMF)—interrupted by other alignments following E-W (Marilópez Fault, MF) and NW-SE (Madre de las Marismas Fault, MMF) directions generate relative movements that can account for the geomorphological anomalies that are found in the sediments and landforms of the present.

The oldest Holocene formations on the surface date from 4706-4071 cal. yr BP and are located north of the TCMF line; south of this fault, by contrast, the visible formations are c. 2000 cal. yr BP old or younger. This terrain south of the TCMF line appears to

have tilted. The tilting must have taken place mostly in the years from c. 4000 to 2000 cal. yr BP, when the littoral system developed toward the centre of the basin as a series of sedimentary sequences of retrogradation and aggradation within a context of sea-level rise because of the subsidence. In those years the estuary would have been far more exposed than now to the dynamics of the sea and thereby more prone to high-energy events such as storm surges and tsunamis and other marine inputs. The strong subsidence in the centre of the basin explains the apparent interruption in the archaeological record of the littoral system that affects pre-Roman and older periods in the Doñana spit. The corresponding Holocene formations underlying the seemingly missing anthropogenic remains sit several metres below the surface. In the spit of La Algaida, on the left-hand side of the Guadalquivir estuary, the processes were less pronounced. From c. 2000 cal. yr BP up to the present, the subsidence has remained relatively dormant, thereby inviting progradation of the littoral systems and infilling of the marshland within a context of sea-level stability. During this period the marshland has been more confined and isolated with respect to marine processes.

In summary, there are good reasons for arguing that the evolution of the Holocene formations and features in the Guadalquivir estuary, as compared to other estuaries in the Gulf of Cadiz, has been rather peculiar. Researchers must take this significant difference into account in attempting to determine regional correlations for southern Iberia with respect to archaeology, geomorphological and sedimentary processes, sea-level oscillations, marine inputs (especially tsunamis and storm surges) and climatic trends during the Holocene.

The model of evolution presented recalls those of the evolution of zones of similar geological characteristics in the planet, located near boundaries of tectonic plates, and can therefore join them as a standard of reference for understanding neotectonic processes worldwide. We also hope that our integrated study will offer an adequate geological explanation for the recent geomorphic and sedimentological features observed in the Doñana UNESCO-MAB Reserve.

Acknowledgements

We are indebted to a vast array of Spanish Institutions: Fundación Caja de Madrid, Fundación Doñana 21, Ayuntamiento de Hinojos, Fundación FUHEM, Estación Biológica de Doñana (EBD), Espacio Natural de Doñana (END), Instituto Andaluz del Patrimonio Histórico (IAPH), Delegación de Cultura of Junta de Andalucía in Huelva and Organismo Autónomo Parques Nacionales of Ministerio de Medio Ambiente y Medio Rural y Marino. Without their encouragement and support, the Hinojos Project would never have sailed. The present paper is a product of the Hinojos Project as well as a contribution to the IGCP 526 ("*Risks, resources, and record of the past on the continental shelf*"), 567 ("*Earthquake Archaeology and Palaeoseismology*") and IGCP 588 ("*Preparing for coastal change*"). We thank reviewers and editors for their helpful comments. This is publication nº 53 from CEIMAR Publication Series.

References

Armijo, R., Benkhelil, J., Bousquet, J. C., Estévez, A., Guiraud, R., Montenat, Ch., Pavillon,M. J., Philip, H., Sanz de Galdeano, C., Viguier, C., 1977. Chapitre III, Les

résultats de l'analyse structurale en Espagne. Groupe de recherche néotectonique de l'Arc de Gibraltar. L'histoire tectonique récent (Tortonien à Quaternaire) de l'Arc de Gibraltar et des bordures de la mer d'Alboran. Bulletin de la Société Géologique de France 7–19, 575–614.

Atwater, B.F., Jiménez-Núñez, H., Vita-Finzi, Cl., 1992. Net Late Holocene emergence despite earthquake-induced submergence, south-central Chile. Quaternary International 15–16, 77-85.

Bolt, B. A., 2003. Earthquakes, fifth edition. New York: W. H. Freeman.

Bonsor, G. E., 1922. El coto de Doña Ana (una visita arqueológica). Madrid: Revista de Archivos, Bibliotecas y Museos.

Bonsor, G. E., 1928. Tartessos: Excavaciones practicadas en el Cerro del Trigo, término de Almonte (Huelva). Madrid: Junta Superior de Excavaciones y Antigüedades.

Borrego, J., Ruiz, F., Morales, J. A., Pendón, J., González-Regalado, M., 1999. The Holocene transgression into the estuarine central basin of the Odiel River Mouth (Cadiz Gulf, SW Spain): Lithology and biological assemblages. Quaternary Science Review 18, 769-788.

Boski, T., Moura, D., Veiga-Pires, C., Camacho, S., Duarte, D., Scott, D. B., Fernández, S. G., 2001. Postglacial sea-level rise and sedimentary response in the Guadiana Estuary, Portugal/Spain border. Sedimentary Geology 150, 103–121.

Campos, J. M., Borja, F., Gómez-Toscano, F., García, J. M., Castiñeira, J. (1993): "Medio natural y condiciones de hábitat en las formaciones arenosas de Doñana (Prospección Arqueológica Superficial)". Anuario Arqueológico de Andalucía 1991, II, 235-238. Sevilla.

Campos, J. M., and Gómez-Toscano, F., 1997. La ocupación humana entre los tramos bajos del Guadiana y el Guadalquivir : su incidencia en la costa holocena. In : J. Rodríguez-Vidal (ed.), Cuaternario ibérico, 305-313. Huelva: Universidad de Huelva.

Campos, J. M., Gómez-Toscano, A., Vidal, N. O., Pérez, J. A., Gómez, C., 2002. La factoría romana de El Cerro del Trigo (Doñana, Almonte, Huelva). Anuario Arqueológico de Andalucía 1999, III-1, 330-348. Sevilla.

Campos, M. L., 1991. Tsunami hazard on the Spanish coasts of the Iberian Peninsula. Science of Tsunami Hazards 9 (1), 83–90.

Corzo, R., 1984. El santuario de La Algaida; en Cádiz y su provincia. Arte Antiguo. Editorial Gener, Sevilla, 137-171.

Cruse, K., 1979. A review of water well drilling methods. The Quarterly Journal of Engineering Geology 12, 79–95.

Dabrio, C. J., Zazo, C., Lario, J., Goy, J. L., Sierro, F. J., Borja, F., González, J. A., Abel Flores, J., 1999. Sequence stratigraphy of Holocene incised-valley fills and coastal evolution in the Gulf of Cadiz (southern Spain). Geologie en Mijnbouw 77, 263–281.

Dabrio, C. J., Zazo, C., Goy, J. L., Sierro, F. J., Borja, F., Lario, J., González, J. A., Flores, J. A., 2000. Depositional history of estuarine infill during the Late Pleistocene-Holocene postglacial transgression. Marine Geology 162, 381–404.

Feagín, R. A., Yeager, K. M., Brunner, C. A., Paine, J. G., 2013. Active fault motion in a coastal wetland: Matagorda, Texas. Geomorphology (199), 150-159.

Fernández Amador de los Ríos, J., 1925. Atlántida: Estudio arqueológico, histórico y geográfico. Zaragoza: Athenaeum.

Flores-Hurtado, E. (1993). Tectónica reciente en el margen ibérico suroccidental. Tesis Doctoral. Universidad de Huelva, 458.

Gómez-Ponce, C., Borja, F., Lagóstena-Barrios, L., López-Amador, J. J., Ruiz, J. A., Borja, C., 1997. Primeras fases de la evolución de la flecha litoral de Valdelagrana (El Puerto de Santa María, Cádiz): Datos arqueológicos. In: Rodríguez-Vidal, J. (ed.), Cuaternario ibérico, 165–167. Huelva: Universidad de Huelva.

Goy, J. L., Zazo, C., Dabrio, C. J., Lario, J., 1994. Fault-controlled shifting shorelines in the Gulf of Cadiz since 20 Ky BP. Abstract Volume, 1st symposium Atlantic Iberian Continental Margin, Lisbon, p. 24.

Goy, J. L., Zazo, C., Dabrio, C. J., Lario, J., Borja,F., Sierro, F. J., Flores, J. A., 1996. Global and regional factors controlling changes of coastlines in southern Iberia (Spain) during the Holocene. Quaternary Science Reviews 15, 773–780.

Goy, J. L., Zazo, C., Dabrio, C. J., 2003. A beach-ridge progradation complex reflecting periodical sea-level and climate variability during the Holocene (Gulf of Almeria, Western Mediterranean). Geomorphology 50, 251–268.

Gutscher, M.A., Malod, J., Rehault, J.P., Contrucci, I., Klingelhoefer, F., Mendes-Victor, L., Spakman, W., 2002. Evidence for active subduction beneath Gibraltar. Geology 30 (12), 1071–1074.

Iribarren, L., Vergés, J., Camurri, F., Fullea, J., Fernández, M., 2007. The structure of the Atlantic–Mediterranean transition zone from the Alboran Sea to the Horseshoe Abyssal Plain (Iberia–Africa plate boundary). Marine Geology. 243, 97–119.

Jackson, N. L., 2013. Estuaries. Treatise on Geomorphology 10, 308-327.

Kennedy, D. M., 2011. Tectonic and Geomorphic Evolution of Estuaries and Coasts Reference Module in Earth Systems and Environmental Sciences, from: Treatise on Estuarine and Coastal Science 1, 37-59.

Kristensen, P., Heier-Nielsen, S., Hylleberg, J., 1995. Late Holocene salinity fluctuations in Bjornsholm Bay, Limfjorden, Denmark, as deduced from micro- and macrofossil analysis. Holocene 5, 313-322.

Kühne, R. W., 2004. A location for 'Atlantis'? Antiquity 78 (300).

Lario, J., Zazo, C., Dabrio, C. J., Somoza, L., Goy, J. L., Bardají, T., Borja, F., 1995. Record of recent Holocene sediment input on spit bars and deltas of South Spain. 17, Special Issue, 241–245.

Lario, J., Zazo, C., Plater, A.J., Goy, J.L., Dabrio, C.J., Borja, F., Sierro, F.J., Luque, L., 2001. Particle size and magnetic properties of Holocene estuarine deposits from the Doñana National Park (SW Iberia): evidence of gradual and abrupt coastal sedimentation. Zeitschrift für Geomorphologie 45, 33-54.

Lario J., Zazo, C., Goy, J. L., Silva, P. G., Bardají, T., Cabero, A., Dabrio, C. J., 2011. Holocene palaeotsunami catalogue of SW Iberia. Quaternary International 242, 196-200.

López-Sáez, J. A., Pérez-Díaz, S., Alba-Sánchez, A., 2011. Antropización y agricultura en el Neolítico de Andalucía Occidental a partir de la palinología. Menga, Revista de Prehistoria de Andalucía 2, 73-86.

Maldonado, A., Somoza, L., Pallarés, L., 1999. The Baetic orogen and the Iberian–African boundary in the Gulf of Cadiz: Geological evolution (central North Atlantic). Mar. Geol. 155, 9–43.

Mastronuzzi, G., Sansó, P., 2012. The role of strong earthquakes and tsunami in the Late Holocene evolution of the Fortore River coastal plain (Apulia, Italy): A synthesis. Geomorphology 138 (1): 89-99

Mauduit, T., Brun, J.P., 1998. Growth fault/rollover systems: birth, growth, and decay. Journal of Geophysical Research 103, 18119–18136.

Mariana, J., 1852-1853. Historia general de España [First edition in 1601]. Madrid: Garpar y Roig.

Medialdea, T., Somoza, L., Pinheiro, L. M., Fernández-Puga, M. C., Vázquez, J. T., León, R., Ivanov, M. K., Magalhaes, V., Díaz-del-Río, V., Vegas, R., 2009. Tectonics and mud volcano development in the Gulf of Cádiz. Marine Geology 261, 48-63.

Menanteau, L., 1979. Les Marismas du Guadalquivir: Exemple de transformation d'un paysage alluvial au cours du Quaternaire récent. Thèse 3^{e} cycle. Université de Paris-Sorbonne, 252 p.

Morton, R.A., Gelfenbaum, G., and Jaffe, B.E., 2007. Physical criteria for distinguishing sandy tsunami and storm deposits using modern examples. Sedimentary Geology 200, 184-207.

Muhs, D.R., Rockwell, T.K., Kennedy, G.L., 1992. Late quaternary uplift rates of marine terraces on the Pacific coast of North America, southern Oregon to Baja California sur. Quaternary International 15–16, 121-133

Nebrija, E. A., 1550. Rerum a Fernando et Elisabe Hispaniarum felicissimis regibus gestarum decades duae. Granada: Xantus et Sebastianus Nebrissensis.

Nelson, A. R., Kelsey, H.M., Witter, R. C., 2006. Great earthquakes of variable magnitude at the Cascadia subduction zone. Quaternary Research 65 (3), 354-365.

Nichol, S. L., Goff, J. R., Devoy, R. J. N., Changué-Goff, C., Hayward, B. and James, I., 2007. Lagoon subsidence and tsunami on the West Coast of New Zealand. Sedimentary Geology, 200, 248-262.

Ota, Y. and Yamaguchi, M., 2004. Holocene coastal uplift in the western Pacific Rim in the context of late Quaternary uplift. Quaternary International 120 (1), 105-117.

Pozo, M., Ruiz, F., Carretero, M. I., Rodríguez-Vidal, J., Cáceres, L. M., Abad, M., González-Regalado, M. L., 2010. Mineralogical assemblages, geochemistry and fossil associations of Pleistocene-Holocene complex siliciclastic deposits from the Southwestern Doñana National Park (SW Spain): A palaeoenvironmental approach. Sedimentary Geology 225, 1-18.

Rey, J. and Fumanal, M. P., 1996. The Valencian coast (Western Mediterranean): Neotectonics and geomorphology. Quaternary Science Reviews 15 (8-9), 789-802.

Rodríguez-Ramírez, A., 1998. Geomorfología del Parque Nacional de Doñana y su entorno. Madrid: Organismo Autónomo Parques Nacionales del Ministerio de Medio Ambiente, 146 p.

Rodríguez-Ramírez, A., Rodríguez-Vidal, J., Cáceres, L., Clemente, L., Belluomini, G., Manfra, L., Improta, S., de Andrés, J. R., 1996. Recent coastal evolution of the Doñana National Park (S. Spain). Quaternary Science Reviews 15, 803–809.

Rodríguez-Ramírez, A., Cáceres, L., Rodríguez-Vidal, J., Cantano, M., 2000. Relación entre clima y génesis de crestas/surcos de playa en los últimos cuarenta años (Huelva, Golfo de Cádiz). Revista de Cuaternario y Geomorfología 14, 109–113.

Rodríguez-Ramírez, A., Ruiz, F., Cáceres, L. M., Rodríguez-Vidal, J., Pino, R., Muñoz, J. M., 2003. Analysis of the recent storm record in the south-western Spain coast: implications for littoral management. The Science of the Total Environment 303: 189-201.

Rodríguez-Ramírez, A., and Yáñez, C. M., 2008. Formation of chenier plain of the Doñana marshland (SW Spain): Observations and geomorphic model. Marine Geology 254, 187-196.

Rodríguez-Ramírez, A., Flores, E., Contreras, C., Villarías-Robles, J. J. R., Celestino-Pérez, S., León, A., 2012. Indicadores de actividad neotectónica durante el Holoceno reciente en el P. N. de Doñana (SO, España). In Avances de la geomorfología en España, 2010-2012: Actas de la XII Reunión Nacional de Geomorfología, Santander, 17-20 septiembre 2012, A. González-Díez (coordinador) and A. González-Díez *et al*. (eds.), 289-292. Santander: Publican, Ediciones de la Universidad de Cantabria.

Rodríguez-Vidal, J., Ruiz, F., Cáceres, L.M., Abad, M., González-Regalado, M.L., Pozo, M., Carretero, M.I., Monge, A.M., Gómez, F., 2011. Geomarkers of the 218–209 BC Atlantic tsunami in the Roman Lacus Ligustinus (SW Spain): a palaeogeographical approach. Quaternary International 242, 201–212.

Rosenbaum, G., Lister, G.S., Duboz, C., 2002. Relative motions of Africa, Iberia and Europe during Alpine orogeny. Tectonophysics 359, 117–129.

Royden, L.H., 1993. Evolution of retreating subduction boundaries forms during continental collision. Tectonics 12 (3), 629–638.

Ruiz, F., Rodríguez-Ramírez, A., Cáceres, L. M., Rodríguez-Vidal, J., Carretero, M. I., Clemente, L., Muñoz, J. M., Yáñez, C., 2004. Late Holocene evolution of the southwestern Doñana National Park (Guadalquivir Estuary, SW Spain): A multivariate approach. Palaeogeography, Palaeoclimatology, Palaeoecology 204, 47–64.

Ruiz, F., Rodríguez-Ramírez, A., Cáceres, L., Rodríguez Vidal, J., Carretero, M.I., Abad, M., Olías, M., Pozo, M., 2005. Evidences of high-energy events in the geological record: Mid-Holocene evolution of the southwestern Doñana National Park (SW Spain). Palaeogeography, Palaeoclimatolology, Palaeoecology 229, 212–229.

Salvany, J. M., 2004. Tilting neotectonics of the Guadiamar drainage basin, SW Spain. Earth Surface Processes and Landforms 29, 145–160.

Salvany, J. M., and Custodio, E., 1995. Características litoestratigráficas de los depósitos pliocuaternarios del bajo Guadalquivir en el área de Doñana: implicaciones hidrogeológicas. Revista de la Sociedad Geológica de España 8, 21–31.

Salvany, J. M., Larrasoaña, J. C., Mediavilla, C., Rebollo, A., 2011. Chronology and tectono-sedimentary evolution of the Upper Pliocene to Quaternary deposits of the lower Guadalquivir foreland basin, SW Spain. Sedimentary Geology 241, 22-39.

Santos, L., Sánchez-Goñi, M. F., Freitas, M. C., Andrade, C., 2003. Climatic and environmental changes in the Santo André coastal area (SW Portugal) during the last 15,000 years. In: Ruiz Zapata, B., Dorado, M., Valdeolmillos, A., Gil, M.J., Bardají, T., Bustamante, I. and Martínez (Eds.), Quaternary climatic changes and environmental crises in the Mediterranean Region, 175–179.

Schulten, A., 1945. Tartessos, 2nd Spanish edition [Original German edition in 1921]. Madrid: Espasa-Calpe.

Shennan, I., Hamilton, S., 2006. Co-seismic and pre-seismic subsidence associated with great earthquakes in Alaska. Quaternary Science Reviews 25 (1–2), 1-8.

Soares, A. M. M., Martins, J. M .M., 2010. Radiocarbon dating of marine samples from Gulf of Cadiz: The reservoir effect. Quaternary International 221, 9-12.

Sorrel, P., Bernadette, T., Demory, F., Delsinne, N., Mouazé, D., 2009. Evidence for millennial-scale climatic events in the sedimentary infilling of a macrotidal estuarine system, the Seine estuary (NW France). Quaternary Science Reviews 28 (5–6), 499-516.

Stevenson, A. C., and Harrison, J., 1992. Ancient forest in Spain: A model for land use and dry forest management in South-west Spain from 4000 BC to 1900 AC. Proceedings of the Prehistoric Society 58, 227-247.

Stuiver, M., and Reimer, P. J., 1993. Radiocarbon calibration program. Rev.4.2. Radiocarbon 35, 215–230.

Stuivert, M., Reimer, P. J., Bard, E., Beck, J. W., Burr, G. S., Hughen, K. A., Kromer, B., McCormac, F. G., v .d. Plicht, J., Spurk, M., 1998. INTCAL98 radiocarbon age calibration, 24,000–0 cal BP. Radiocarbon 40, 1041–1083.

Torelli, L., Sartori, R., Zitellini, N., 1997. The giant chaotic body in the Atlantic Ocean off Gibraltar: new results from a deep seismic reflection survey. Mar. Pet. Geol. 14, 125–138.

Uluğ, A., Duman, M., Ersoy, S., Özel, E. & Avci, M., 2005. Late Quaternary sea-level change, sedimentation and neotectonics of the Gulf of Gökova: Southeastern Aegean Sea. Marine Geology 221(1–4), 381-395.

Viguier, C., 1977. Les grands traits de la tectonique du basin néogène du Bas Guadalquivir. Boletín Geológico Minero 88, 39–44.

Vizcaíno, A., Gràcia, E., Pallàs, R., García-Orellana, J., Escutia, C., Casas, D., Willmott, V., Díez, S., Asioli, A., Dañobeitia, J.J., 2006. Sedimentology, physical properties and ages of mass-transport deposits associated to the Marquês de Pombal Fault, Southwest Portuguese Margin. Norwegian Journal of Geology 86, 177-186.

Vött, A., 2007. Relative sea level changes and regional tectonic evolution of seven coastal areas in NW Greece since the mid-Holocene. Quaternary Science Reviews 26, 894–919.

Yeager , K. M., Brunner, C. A., Kulp, M. A., Fischer, D., Rusty A. Feagin, R. A., Schindler , K. J., Prouhet, J., Gopal Bera, G., 2012. Significance of active growth faulting on marsh accretion processes in the lower Pearl River, Louisiana. Geomorphology (153-154), 127-143 .

Zazo, C., Goy, J. L., Somoza, L., Dabrio, C. J., Belluomini, G., Improta, S., Lario, J., Bardaji, T., Silva, P. G., 1994. Holocene sequence of sea-level fluctuations in relation to

climatic trends in the Atlantic–Mediterranean linkage coast. Journal of Coastal Research 10, 933–945.

Zazo, C., Dabrio, C. J., González, J., Sierro, F., Yll, E. I., Goy, J. L., Luque, L., Pantaleón-Cano, J., Soler, V., Roure, J. M., Lario, J., Hoyos, M., Borja, F., 1999a. The records of the later glacial and interglacial periods in the Guadalquivir marshlands (Marilopez drilling, SW Spain). Geogaceta 26, 119–122.

Zazo, C., Dabrio, C. J., Borja, J., Goy, J. L., Lézine, A. M., Lario, J., Polo, M. D., Hoyos, M., Boersma, J.R., 1999b. Pleistocene and Holocene aeolian facies along the Huelva coast (southern Spain): Climatic and neotectonic implications. Geologie en Mijnbouw 77, 209–224.

Zazo, C., Silva, P.G., Goy, J.L., Hillaire-Marcel, C., Ghaleb, B., Lario, J., Bardají, T., González, A., 1999c. Coastal uplift in continental collision plate boundaries: Data from the Last Interglacial marine terraces of the Gibraltar Strait area (south Spain). Tectonophysics 301 (1–2), 95-109.

Zazo, C., Mercier, N., Silva, P. G., Dabrio, C. J., Goy, J. L., Roquero, E., Soler, V., Borja, F., Lario, J., Polo, D., Luque, L., 2005. Landscape evolution and geodynamic controls in the Gulf of Cadiz (Huelva coast, SW Spain) during the Late Quaternary. Geomorphology 68, 269–290.

Zazo, C., 2006. Cambio climático y nivel del mar: la Península Ibérica en el contexto global. Cuaternario y Geomorfología 20 (3–4), 115–130.

Zazo, C., Dabrio, C.J., Goy, J.L., Lario, J., Cabero, A., Silva, P.G., Bardají, T., Mercier, N., Borja, F., Roquero, E., 2008. The coastal archives of the last 15 Ka in the Atlantic–Mediterranean Spanish linkage area: sea level and climate changes. Quaternary International 181 (1), 72–87.

Figure captions

Figure 1.- Study Area. TLF.- Torre del Loro Fault. GMF.- Guadiamar-Matalascañas Fault. HBF.- Hato Blanco Fault. BGF.- Lower Guadalquivir Fault. TCMF.- Torre Carbonero-Marilópez Fault. MF.- Marilópez Fault. MMF.- Madre de las Marismas Fault.

Figure 2.- Correlation of prograding units exposed between the Tinto-Odiel, Guadalquivir, and Guadalete estuaries. Data from Zazo et al. (1994), Rodríguez-Ramírez et al. (1996), Goy et al. (1996), Dabrio et al. (2000) and Zazo et al. (2006, 2008).

Figure 3.- Most visible alignments and location of topographic sections (A-B and C-D) on a 1956 orthophotograph.

Figure 4.- Topographic sections C-D and A-B and abrupt topographic change.

Figure 5.- A relic of old marshland, north of the Carrizosa-Vetalarena sandy ridge.

Figure 6.- Composition and stratigraphy of the analyzed cores.

Figure 7.- Tectono-sedimentary/geomorphic evolution of the Guadalquivir estuary. A.- Holocene transgression on the estuary . B.- Activation of TCMF. Strong marine input on the estuary, subsidence, overwash over ADF, and destruction of human settlements C.- Sedimentary infilling by fluvial input and evolution from lagoon to tidal marsh. D. Development of littoral progradational units and sedimentary infilling of estuary to freshwater marsh.

Figure 8.- Correlation between morphodynamics, sedimentary evolution and human occupation.

Figure 9.- Lateral and vertical succession of sedimentary bodies in the Guadalquivir palaeoestuary.

Table captions

Table 1.- Location of the studied cores and elevation with respect to the MSL. (a) UTM coordinates, Zone 29N. (b) Boreholes drilled by IGME (Geological and Mining Institute of Spain).

Table 2.- Dates of the different formations. B.- Beta Analytic Laboratory (Miami, USA). CNA.-Centro Nacional de Aceleradores (Seville, Spain). DAMS.- Accium BioSciences Accelerator Mass Spectrometry Lab (Seattle, USA). CX.- Geochron Laboratories, Krueger Enterprises, Inc., (Cambridge, USA). ([a])Rodríguez-Ramírez *et*

al., 1996. ([b])Rodríguez Ramírez & Yáñez, 2008. ([c])Pozo *et al*., 2010. ([d])Salvany *et al.*, 2011. ([e])Zazo *et al.*, 1999a. ([f])Rodríguez-Vidal et al., (2011). Samples: T.- Transported. PT.-Poorly transported. NT.-Not transported.

Table 3.- Outline of the sedimentary formations under study.

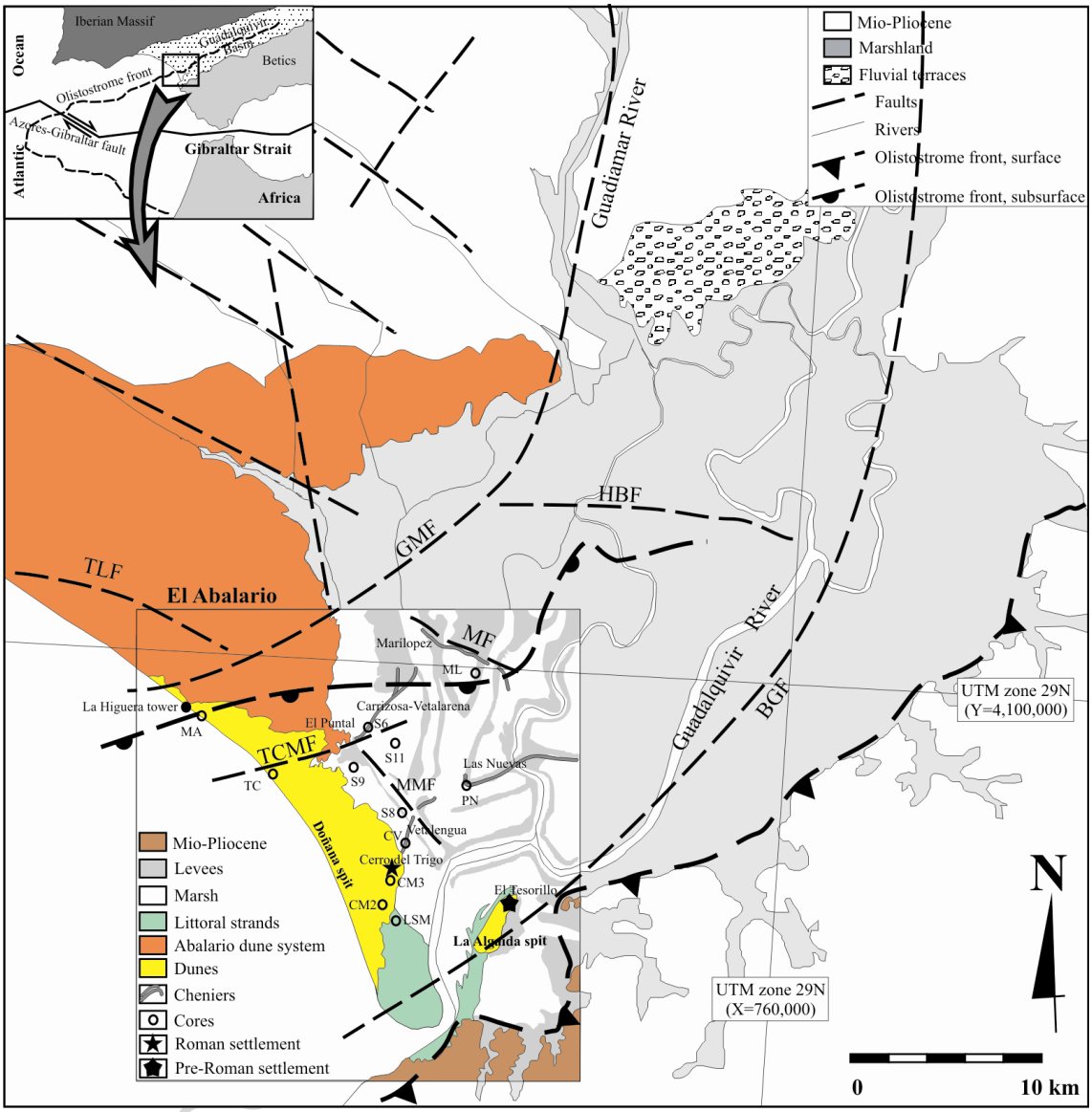

Figure 1

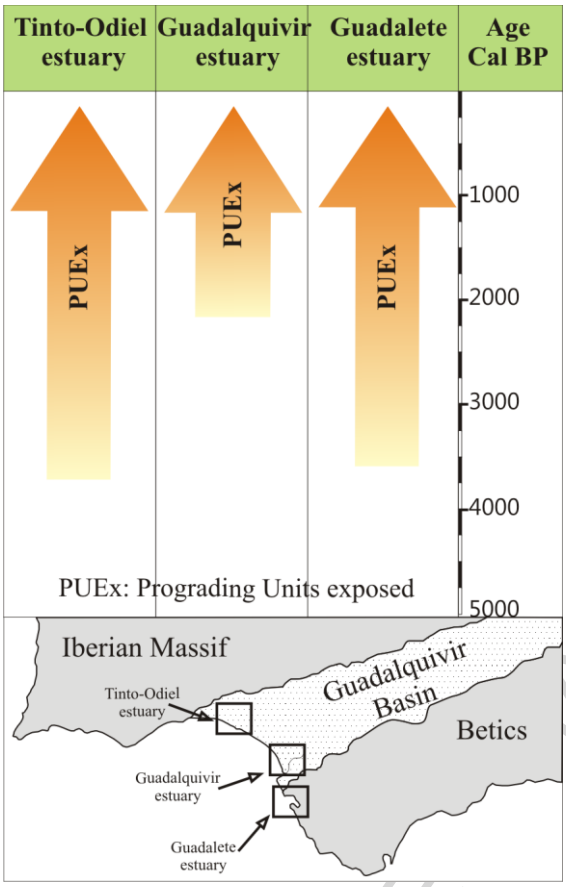

Figure 2

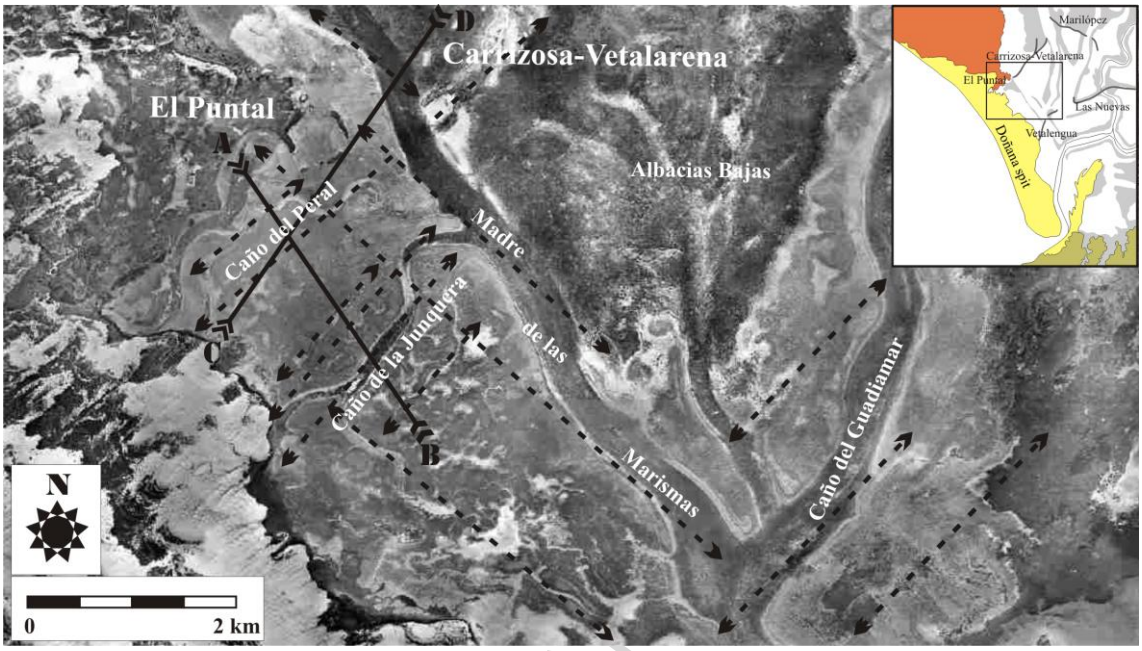

Figure 3

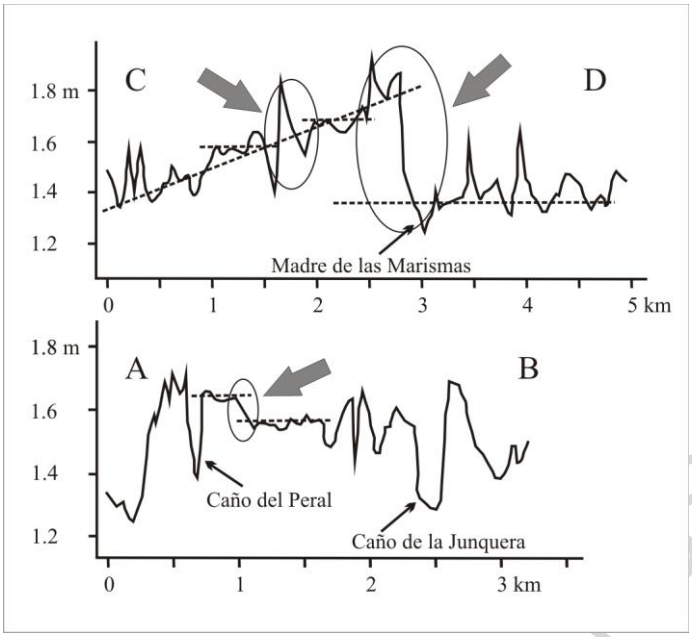

Figure 4

Figure 5

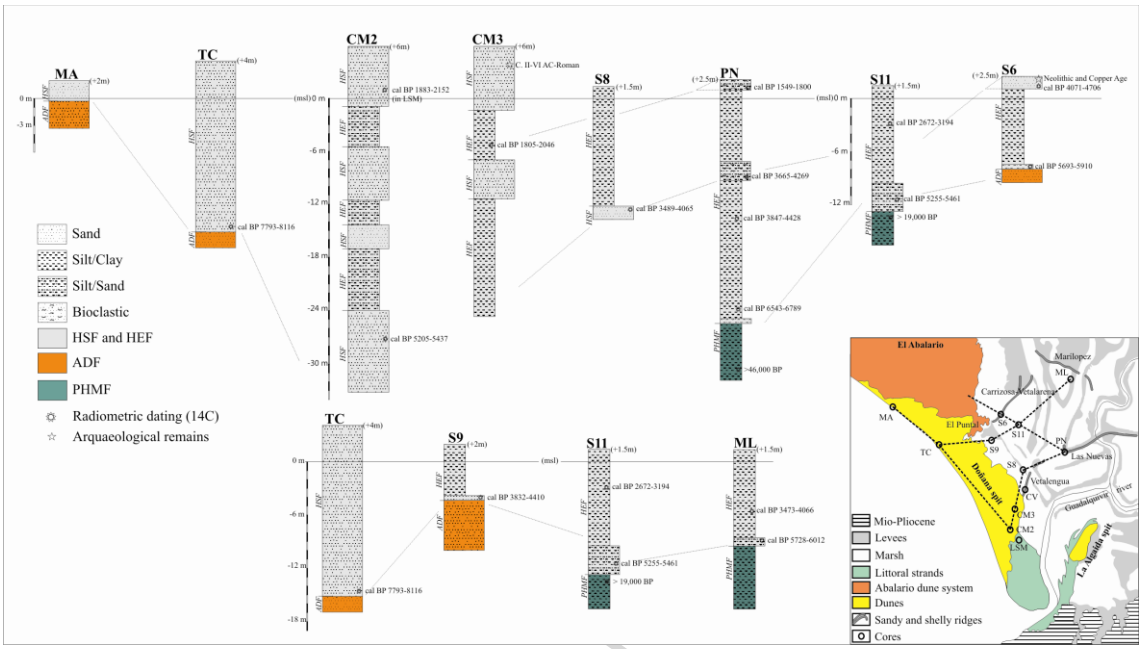

Figure 6

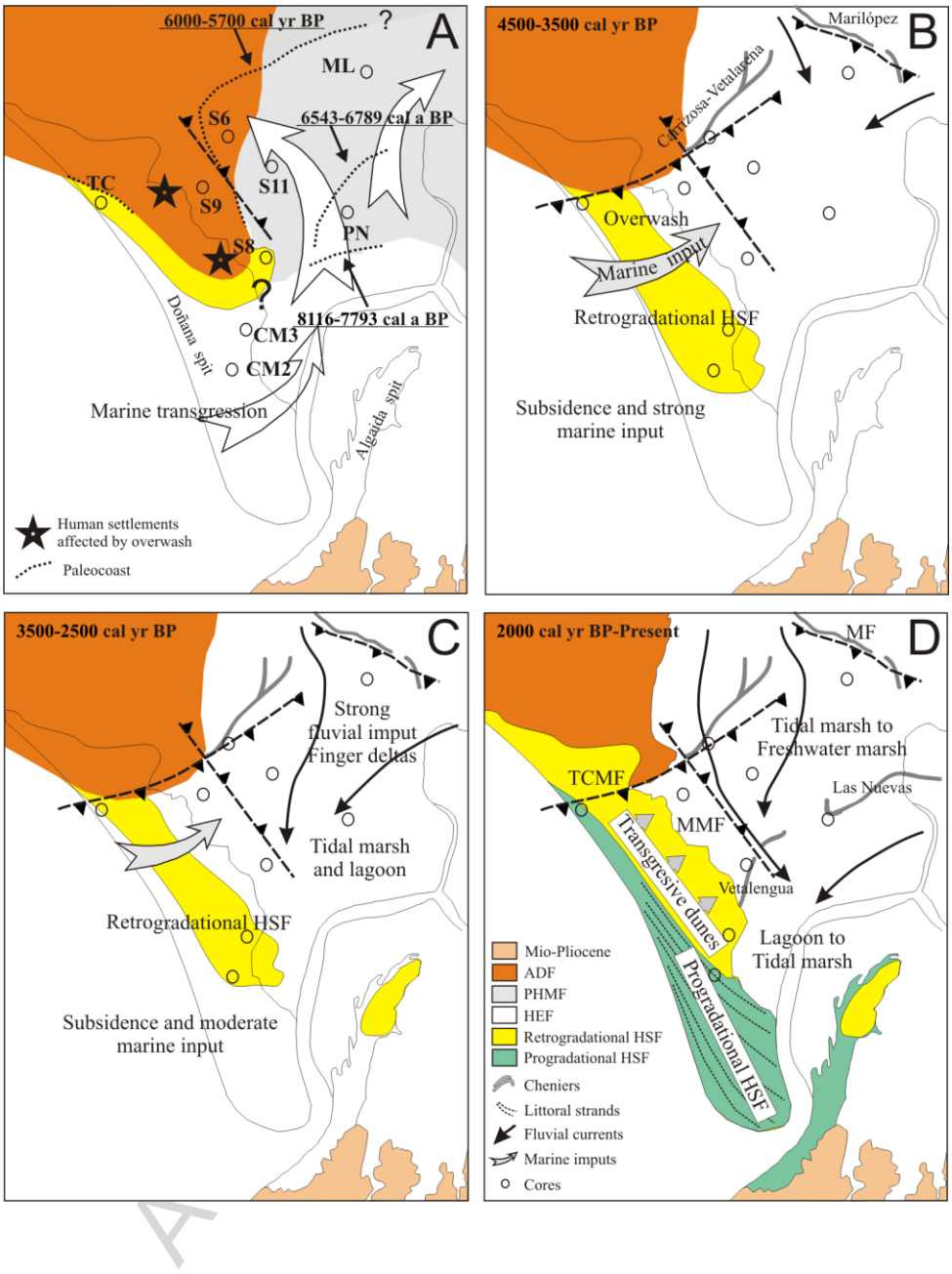

Figure 7

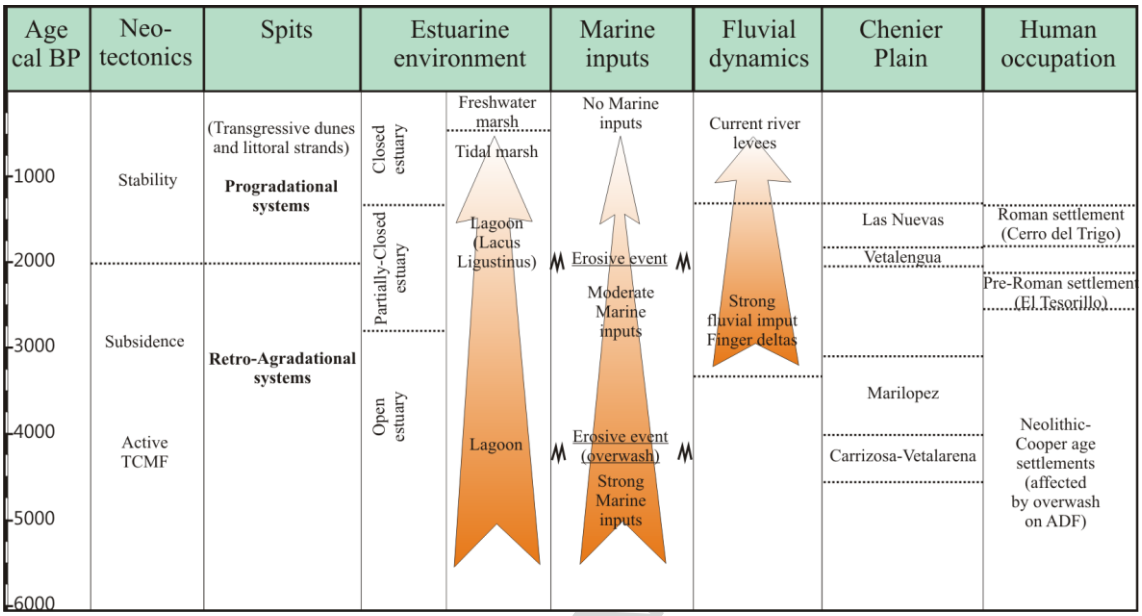

Figure 8

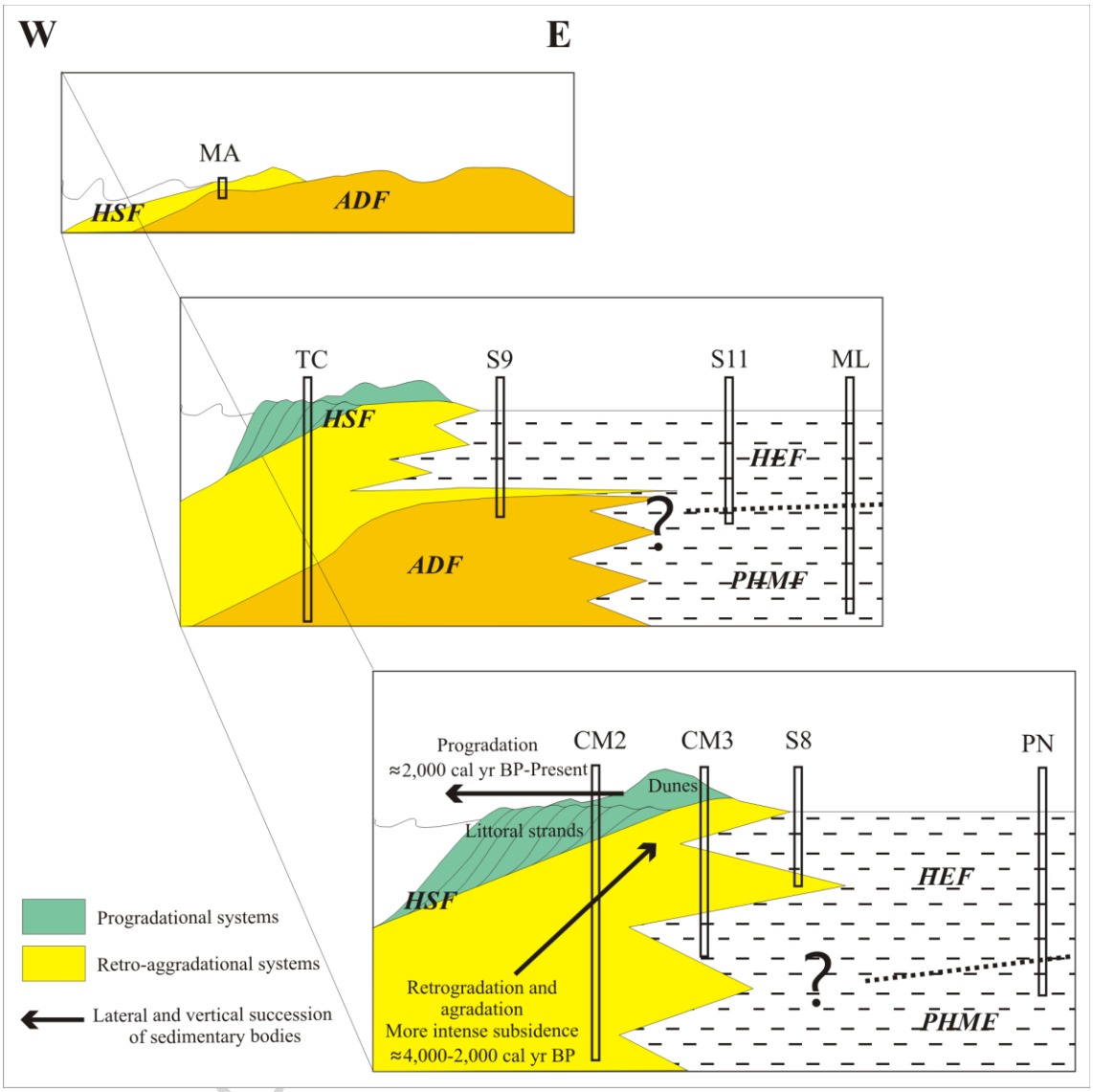

Figure 9

Table 1

Core	**X (UTM[a])**	**Y(UTM[a])**	**Z (m)**
[b]TC	724,502	4,091,592	+4
[b]CM2	732,572	4,083,562	+6
[b]CM3	732,629	4,085,625	+6
[b]ML	737,222	4,100,866	+1.5
[b]PN	737,503	4,092,111	+2.5
S6	730,636	4,095,665	+2.5
S8	732,979	4,090,362	+1.5
S9	730,173	4,092,611	+2
S11	731,841	4,094,679	+1.5
MA	720,208	4,095,845	+2

Table 2

Ref. Lab.	Core	Depth	Sample	^{14}C yr (BP)	δ^{13}C‰	^{14}C cal. yr 2σ (BP)	ΔR (^{14}C yr)
B-287646	S6	-0.5m	*Cerastoderma edule* (PT)	4370±40	-1.8	4071-4706	100±100
B-284999	S6	-10m	*Glycimeris* sp. (PT)	5300±40	1.4	5693-5910	−135±20
B-285003	S8	-14m	*Tellina tenuis* (NT)	3920±40	1.0	3489-4065	100±100
B-285004	S9	-6m	Cerastoderma edule (NT)	4180±40	0.6	3832-4410	100±100
B-285006	S11	-4m	Cerastoderma edule (NT)	3190±40	-2.5	2672-3194	100±100
B-285007	S11	-11.5m	*Tellina tenuis*(NT)	4860±40	-0.3	5255-5461	−135±20
B-285008	S11	-13m	Cerastoderma edule (PT)	19360±80	-25.2	Uncalibrated	
DAMS 1217-177	TC	-19,8m	*Venerupis decussatus* (PT)	7349±68	1.6	7793-8116	−135±20
CNA-273	LSM	-0,5m	*Glycimeris* sp. (T)	2260±45	-1.1	1883-2152	−135±20
[a]B-88016	CV	-0,5m	Cerastoderma edule (NT)	2230±60	--	1825-2149	−135±20
DAMS-1217-178	CM2	-33m	*Tellina tenuis*(PT)	4820±31	-5.9	5205-5437	−135±20
[f]B-228874	CM3	-11m	shell	2170±40	--	1805-2046	−135±20
[b]B-154079	PN	-0.5m	*Cerastoderma edule* (PT)	1960±40	-0.9	1549-1800	−135±20
[c]B-228881	PN	-10.8m	shell	4060±40	--	3665-4269	100±100
[c]B-228885	PN	-14.1m	shell	4200±40	--	3847-4428	100±100
[c]B-228882	PN	-26.1m	shell	6090±40	--	6543-6789	−135±20
[d] BA	PN	-35.5m	Peat	>46,000	-27.5	Uncalibrated	
[e]CX-238339	ML	-7.3m	shell	3915±50	-1.9	3473-4066	100±100
[e]CX-23840-A	ML	-10.8m	shell	5370±50	0.4	5728-6012	−135±20
[e]CX-23841	ML	-27m	Shell	>47,000	-5.8	Uncalibrated	

Table 3

Formations		Lithology	Mineralogy	Paleontology (macrofossil)	Others	Interpretation
PHMF		Silts: 60-75% Clay: 20-25% Sand: 2-5%	Quartz: 6-10% Feldspar: 2-4% Calcite: 15-35% Dolomite: 0-7%	Absent	Lamination Burrowing, roots Carbonate nodules Oxidation	Freshwater to brackish marsh
ADF		Silts: 5-20% Clay: 1-4% Sand: 75-90% Well sorted	Quartz: 75-95% Feldspar: 5-14% Filosilicates: 8-10% Dolomite: 2-3%	Absent	Crossbedding Oxidation Bioturbation, roots Peat bogs	Dune systems
HEF		**Clayey Silt facies:** Silts: 65-70% Clay: 20-30% Sand: 0-6%	Quartz: 75-95% Feldspar: 5-14% Filosilicates: 8-10% Dolomite: 2-3%	Estuarine species Toward the top, continental and freshwater species. Little or no transport	Burrowing Lamination	Estuary confined High fluvial inputs Tidal to freshwater marsh
		Sandy silt facies: Silts: 30-40% Clay: 10-15% Sand: 10-30%	Quartz: 10-20% Filosilicates: 30-50% Calcite: 15-20%	Estuarine species and some remains of transported marine species	Burrows, roots, and lamination	Open estuary Coastal lagoon with marine input
		Sandy layers facies: Silts: 25-40% Clay: 5-10% Sand: 40-70%	Quartz: 50-95% Feldspar: 10% Filosilicates: 10-40% Dolomite: 10-15%	Wide diversity of species of malacofauna (marine and estuarine.) High transport	Coarse boulders Lithoclasts Erosive base	Marine input High energy events Open estuary
		Bioclast layers facies: Silts: 40-60% Clay: 25-30% Sand: 10-30%	Quartz: 10-20% Filosilicates: 50-70% Calcite: 15-25%	Mostly *Cerastoderma edule* and *Crassostrea angulata*	Erosive base Littoral strand morphology	Cheniers
		Dune facies Sand: 100%. Well sorted and rounded Mean grain size	Quartz: 70-85% Filosilicates: 15-25% Feldspar: 5-10%	Absent	Crossbedding	Dune systems of the spit barriers

		of 125 to 500µm				
HSF		**Beach facies** Fine-to-coarse-grained sands, badly sorted.	Quartz: 40-55% Filosilicates: 10-20% Feldspar: 15-25% Calcite: 10-15%	Wide diversity of species of marine malacofauna, rather deteriorated by reworking	Lamination, crossbedding	Beach

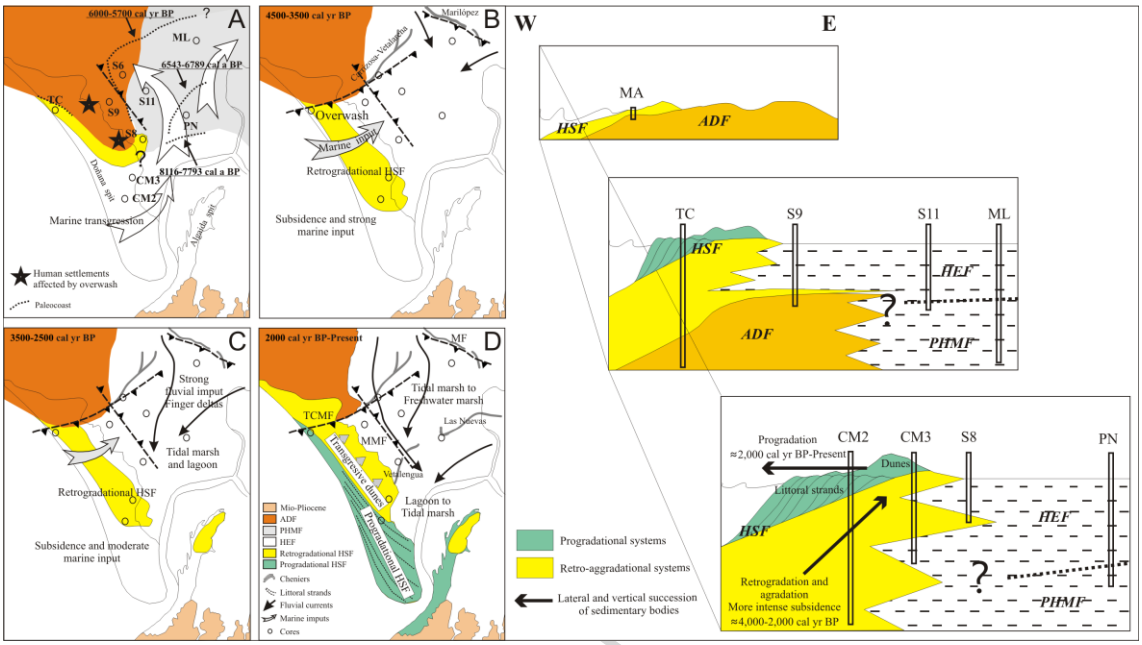

Graphical abstract

Highlights

New data are provided for the Holocene sedimentary infilling.

New data are provided for the Holocene geomorphic evolution.

Neo-tectonic activity strongly conditions Holocene sedimentation.

The geomorphology and the stratigraphic sequence of the basin are defined.